A NEW ASYMPTOTIC PRESERVING SCHEME BASED ON MICRO-MACRO FORMULATION
FOR LINEAR KINETIC EQUATIONS IN THE DIFFUSION LIMIT

Mohammed Lemou[1], Luc Mieussens[2]

Abstract. We propose a new numerical scheme for linear transport equations. It is based on a decomposition of the distribution function into equilibrium and non-equilibrium parts. We also use a projection technique that allows to reformulate the kinetic equation into a coupled system of an evolution equation for the macroscopic density and a kinetic equation for the non-equilibrium part. By using a suitable time semi-implicit discretization, our scheme is able to accurately approximate the solution in both kinetic and diffusion regimes. It is asymptotic preserving in the following sense: when the mean free path of the particles is small, our scheme is asymptotically equivalent to a standard numerical scheme for the limit diffusion model. A uniform stability property is proved for the simple telegraph model. Various boundary conditions are studied. Our method is validated in one-dimensional cases by several numerical tests and comparisons with previous asymptotic preserving schemes.

Key words. transport equations, diffusion limit, asymptotic preserving schemes, stiff terms

AMS subject classifications. 65M06, 35B25, 82C80, 41A60

1   Introduction

In neutron transport, radiative transfer, or rarefied gas dynamics, particle systems can be described at different scales. When the mean free path of the particles is large as compared to a macroscopic length, the system is commonly described at a microscopic level by kinetic theory. Even if kinetic equations may contain a very large number of unknowns and variables, the use of modern supercomputers makes it possible realistic simulations. When the mean free path of the particles is small, a macroscopic description—such as diffusion equation in neutron transport and radiative transfer or fluid equations in rarefied gas dynamics—is often accurate enough, and leads to much faster numerical simulations.

Mathematically, one can pass from kinetic to macroscopic models by asymptotic analysis. However, numerically this is a much more challenging problem. Indeed, when the mean free path and the macroscopic reference length differ from several orders of magnitude, the kinetic equation contains stiff terms that make classical numerical methods prohibitively expensive.

[1]IRMAR, CNRS et Université de Rennes 1, France (`mohammed.lemou@univ-rennes1.fr`)

[2]Université de Toulouse; UPS; Institut de Mathématiques; 31062 Toulouse, France (`Luc.Mieussens@math.univ-toulouse.fr`)

For instance for multiscale problems where there are different zones with very different mean free paths, many classical methods cannot be used.

It is of course attractive to use domain decomposition methods with coupling strategies to solve relevant microscopic or macroscopic model wherever it is necessary. For linear transport equations, this has been largely studied, for instance in Bal and Maday [1], Degond and Schmeiser [6], Golse, Jin and Levermore [7], Klar [18], and Klar and Siedow [23], and more recently in Degond and Jin [4].

Another strategy consists in looking for numerical approximations of the kinetic equation that, in some sense, reduce to numerical approximations of the macroscopic equation when the scaling parameter goes to zero, without any prohibitive restriction on the numerical parameters of the method. These methods mimic the asymptotic behavior of the kinetic equation itself and are often called Asymptotic Preserving (AP) schemes. For stationary equations, several space discretizations were for instance studied (for neutron transport) by Larsen, Morel and Miller [26], Larsen and Morel [25], and Jin and Levermore [11, 12]. In these works, it was shown that many classical space discretizations fail to capture the macroscopic (diffusive) regime. Indeed these methods give correct results when the mesh size is smaller that the mean free path, which requires prohibitively fine meshes, while they give uncorrect results with coarser meshes composed of cells larger than the mean free path (so-called optically thick cells in [26]). These authors proposed new discretizations that give an accurate description of the macroscopic regime, even with coarse meshes.

For unstationary problems, the additional difficulty is that usual time explicit discretizations require a very restrictive stability time step constraint that make them useless in the macroscopic regime. On the contrary, time implicit schemes are theoretically uniformly stable, but the size of kinetic problems is generally so large that these schemes are often too expensive. Very recently, two classes of semi-implicit time discretization have been proposed by Klar [19] and Jin, Pareschi and Toscani [16] (see preliminary works in [15, 10] and extensions in [14, 13, 27, 20, 21], and another strategy by Gosse and Toscani [8, 9]). While the space discretization is quite classical (simple finite differences), the time discretization is based on a scale separation of the equation that makes the main stiffness disappear. For the method of [19], the initial data is separated into microscopic and macroscopic components, and the linearity of the kinetic equation is used to evolve the two components separately with a coupled system of equations. For the method of [16], the parity of the collision operator is used to obtain a system of coupled kinetic equations for the odd and even parts of the unknown. Additionally, the relaxation scheme theory [17] is used to remove the stiffness of the equation. In these references, the new methods have been proved to have many interesting properties: they are uniformly stable, uniformly accurate, and are AP.

In this article, we propose a new method that we believe to be more adapted to general frameworks. We use a classical decomposition (called micro-macro decomposition) of the unknown into microscopic and macroscopic components which remains valid at any time. A coupled system of equations is obtained for these two components without any linearity assumption. The decomposition only uses basic properties of the collision operator that are common to most of kinetic equations (namely conservation and equilibrium properties).

Then this system is solved with a suitable semi-implicit method that does not use any time splitting scheme, as opposed to [19, 16]. We mention that this decomposition has also been used to design a new coupling method for kinetic/fluid multiscale problems by Degond, Liu and Mieussens [5], without decomposition domain technique. Also note that similar ideas can be found in the work of Klar and Schmeiser [22] for the radiative heat transfer equation.

Even if our method can be applied to several kind of kinetic equations, this article is restricted to linear equations such as the neutron transport model. We prove that our method is indeed AP: when the scale parameter goes to zero, the limit scheme is a classical scheme for the macroscopic (diffusion) equation. We also exhibit an explicit CFL time step condition in a simple case. We present several numerical tests to validate the approach which is systematically compared to the methods of [19, 16]: the advantages and drawbacks of our method are then discussed. Note that an application of our approach to non-linear equations can be found in [3].

The outline of the article is the following. In section 2, we give a general kinetic equation and two simple examples. The macroscopic diffusion limit is also presented. We then perform the micro-macro decomposition on the equation, which is the key ingredient in the construction of our numerical method. In section 3, the numerical discretization of the kinetic equation following the micro-macro decomposition is detailed, as well as a discretization of the boundary conditions. Then, the numerical scheme is formally proved to be AP. In section 4, a stability analysis is given in a simple case. Various numerical tests are finally presented in section 5.

2   Linear kinetic equations and their diffusion limits

2.1   General setting

We consider the following transport equation in a diffusive scaling

$$\varepsilon \partial_t f + v \cdot \nabla_x f = \frac{1}{\varepsilon} L f + \varepsilon S, \tag{1}$$

with initial data

$$f|_{t=0} = f_{init}, \tag{2}$$

where f is the velocity distribution function of the particles that depends on time $t > 0$, on position $x \in \mathbb{R}^d$, and on velocity $v \in \Omega$. The left-hand side is the convection operator that models the transport of particles along straight lines, while L is a linear operator that models the interactions of particles with the medium, and S is a source and/or production term. The parameter ε measures the "distance" of the system to equilibrium in the system: when ε is small, the system is close to an equilibrium state, while for large ε, the system is far from equilibrium. Both Lf and S are supposed to be bounded with respect to ε.

The velocity space is endowed with a measure μ and we denote by $\langle f \rangle := \int_\Omega f \, d\mu$ the integral of any vector-valued function of v which is μ-measurable. We assume that there

exists a positive function E (called absolute equilibrium state) that does not depend on t and x, such that

$$\langle E \rangle = 0 \quad \text{and} \quad \langle vE \rangle = 0.$$

Then we consider the Hilbert space $L^2(\Omega; E^{-1} d\mu)$ endowed with the following inner product

$$\langle f, g \rangle := \int_\Omega fg E^{-1} d\mu.$$

Now we make the following assumptions on the collision operator L:

- L acts only on the velocity dependence of f (it is local with respect to t and x);

- L is non-positive self-adjoint in $L^2(\Omega; E^{-1} d\mu)$;

- the null space and the rank of L are

$$\mathcal{N}(L) = Span\{E\} = \{f = \rho E, \text{where } \rho := \langle f \rangle\}$$
$$\mathcal{R}(L) = (\mathcal{N}(L))^\perp = \{f \text{ such that } \langle f \rangle = 0\}.$$

From these assumptions, it is easy to obtain the following lemma

Lemma 2.1. *(i) the equation $Lf = g$ with $g \in \mathcal{R}(L)$ has a unique solution f in $\mathcal{R}(L)$. It is denoted by $L^{-1}g$, where L^{-1} is the pseudo-inverse of L on $\mathcal{R}(L)$.*

(ii) the orthogonal projection Π of $L^2(\Omega; E^{-1} d\mu)$ onto $\mathcal{N}(L)$ is defined by

$$\Pi\phi = \langle \phi \rangle E \tag{3}$$

for every ϕ.

The proof if left to the reader.

We describe now two simplified versions of the general kinetic equation (1), which are used throughout this article. The one-group transport equation in slab geometry is such that $d = 1$, the velocity set is the set of cosine angles of the velocities $\Omega = [-1, 1]$, $\mu = \frac{1}{2}dv$ and L is the scattering operator $Lf = \sigma_S(\langle f \rangle - f)$. In this case, the absolute equilibrium state is $E = 1$. It is then classical to prove that L satisfies all the previous properties. The "source" term is $S = -\sigma_A f + G$ that models the absorption and production of particles by the medium. Then equation (1) reads

$$\varepsilon \partial_t f + v \partial_x f = \frac{\sigma_S}{\varepsilon}(\langle f \rangle - f) - \varepsilon \sigma_A f + \varepsilon G, \tag{4}$$

where σ_S and σ_S are scattering and absorption coefficients that may depend on x.

We also consider the simplest version of (1) which is known as the telegraph equation or the one-dimensional Goldstein-Taylor model. It is a discrete kinetic equation in which $d = 1$ and $\Omega = \{-1, 1\}$. It can be obtained by the one-group equation (4) in which dv is the

discrete Lebesgue measure associated with Ω, and with $S = 0$. Note that functions of v are 2-vector valued $f = (f(1), f(-1))$, and set $f = (u, v)$. The telegraph equation then reads

$$
\begin{aligned}
\varepsilon \partial_t u + \partial_x u &= \frac{1}{2\varepsilon}(v - u), \\
\varepsilon \partial_t v - \partial_x v &= \frac{1}{2\varepsilon}(u - v).
\end{aligned}
\tag{5}
$$

Note that this simple system can be put under another classical form by introducing the variables $\rho = \frac{1}{2}(u + v)$ and $j = \frac{1}{2\varepsilon}(u - v)$. We get

$$
\begin{aligned}
\partial_t \rho + \partial_x j &= 0, \\
\varepsilon^2 \partial_t j + \partial_x \rho &= -j.
\end{aligned}
\tag{6}
$$

This form is the basis of the schemes developed in [15, 10, 13, 14].

2.2 Diffusion limit

When ε goes to 0 in (1), it is easy to see that f goes to f_0 which is a solution to $L f_0 = 0$. This means that f converges to an equilibrium state of the form $\rho_0 E$. The diffusion limit is the equation satisfied by the density ρ_0. It is usually obtained by injecting the Hilbert expansion $f = f_0 + \varepsilon f_1 + \varepsilon^2 f_2 + \ldots$ into (1) and then by equalizing terms of same order in ε. Then it is found that $f_0 = \rho_0 E$, and that f_1 is a solution of

$$
v \cdot \nabla_x f_0 = L f_1.
$$

By lemma 2.1, f_1 is found to be $L^{-1}(vE) \cdot \nabla_x \rho_0$. Finally, f_2 exists if and only if ρ_0 satisfies the following diffusion equation (solvability condition)

$$
\partial_t \rho_0 + \nabla_x \cdot (\kappa \nabla_x \rho_0) = \langle S_0 \rangle,
\tag{7}
$$

where

$$
\kappa = \langle v L^{-1}(vE) \rangle
\tag{8}
$$

is the non-positive diffusion coefficient (see [2]).

2.3 The micro-macro decomposition

We propose a slightly different approach which goes in the spirit of the well-known Chapman-Enskog expansion method in the kinetic theory of gases. We emphasize that in the following approach, no approximation is needed and the obtained model is strictly equivalent to the original one. The idea consists in using the following micro-macro decomposition of f:

$$
f = \rho E + \varepsilon g,
\tag{9}
$$

where ρE is the equilibrium part of f defined by

$$\rho = \langle f \rangle, \tag{10}$$

which, in particular, is not the limit of f when ε goes to 0. Then, the non-equilibrium part g satisfies

$$\langle g \rangle = 0, \tag{11}$$

which implies that $g \in \mathcal{R}(L)$.

Now, decomposition (9) is injected into the kinetic equation (1) to obtain

$$\varepsilon E \partial_t \rho + \varepsilon^2 \partial_t g + v \cdot E \nabla_x \rho + \varepsilon v \cdot \nabla_x g = Lg + \varepsilon S. \tag{12}$$

If we integrate this equation on Ω with respect to the measure μ, we find the following continuity equation with a source term

$$\varepsilon \partial_t \rho + \varepsilon \nabla_x \cdot \langle vg \rangle = \varepsilon \langle S \rangle. \tag{13}$$

Then an evolution equation on g is found by applying the orthogonal projection $I - \Pi$ (see point (ii) of lemma 2.1) to (12)

$$\varepsilon^2 \partial_t g + \varepsilon (I - \Pi)(v \cdot \nabla_x g) + v \cdot E \nabla_x \rho = Lg + (I - \Pi)\varepsilon S. \tag{14}$$

Consequently, the micro-macro formulation of (1) is given by equations (13) and (14) which we rewrite as follows

$$\partial_t \rho + \nabla_x \cdot \langle vg \rangle = \langle S \rangle, \tag{15}$$

$$\partial_t g + \frac{1}{\varepsilon}(I - \Pi)(v \cdot \nabla_x g) = \frac{1}{\varepsilon^2} Lg + \frac{1}{\varepsilon}(I - \Pi)S - \frac{1}{\varepsilon^2} v \cdot E \nabla_x \rho. \tag{16}$$

This is the formulation we use in our numerical scheme. It is equivalent to the original kinetic equation, as it is stated in the following proposition.

Proposition 2.1. *(i) If f is a solution of (1) with initial data (2), then $(\rho, g) = (\langle f \rangle, \frac{1}{\varepsilon}(f - \rho E))$ is a solution of (15–16) with the associated initial data*

$$\rho|_{t=0} = \rho_{init} = \langle f_{init} \rangle \quad and \quad g|_{t=0} = \frac{1}{\varepsilon}(f_{init} - \rho_{init}E). \tag{17}$$

(ii) Conversely, if (ρ, g) is a solution of (15)–(16) with initial data (17), then $\langle g \rangle = 0$ and $f = \rho E + \varepsilon g$ is a solution of (1)–(2).

Now we briefly show how the diffusion limit can be readily obtained from this system. From the second relation (16), it is clear (formally) that g converges to $L^{-1}(vE) \cdot \nabla_x \rho_0$ where ρ_0 is the limit of ρ when ε goes to 0. Then passing to the limit into the first relation (15) directly gives the diffusion equation (7).

Similarly, for the simpler case of the one-group transport equation (4), the equivalent micro-macro formulation is

$$\partial_t \rho + \partial_x \langle vg \rangle = -\sigma_A \rho + G, \tag{18}$$

$$\partial_t g + \frac{1}{\varepsilon}(I - \Pi)(v\partial_x g) = -\frac{\sigma_S}{\varepsilon^2} g - \frac{1}{\varepsilon^2} v\partial_x \rho - \sigma_A g. \tag{19}$$

For the telegraph equation (5), f is decomposed into $f = \rho E + \varepsilon g$ where $\rho = \frac{1}{2}(u + v)$, $E = (1, 1)$, and $g = (\alpha, \beta)$, where the property $\langle g \rangle = 0$ now reads $\alpha = -\beta$. The micro-macro system is

$$\partial_t \rho + \partial_x \frac{\alpha - \beta}{2} = 0,$$

$$\partial_t \alpha + \frac{1}{\varepsilon}\partial_x \frac{\alpha + \beta}{2} = -\frac{1}{\varepsilon^2}\alpha - \frac{1}{\varepsilon^2}\partial_x \rho, \tag{20}$$

$$\partial_t \beta - \frac{1}{\varepsilon}\partial_x \frac{\beta + \alpha}{2} = -\frac{1}{\varepsilon^2}\beta + \frac{1}{\varepsilon^2}\partial_x \rho.$$

2.4   Initial and boundary conditions

In view of a practical use of the micro-macro formulation (15)–(16), we consider the initial-boundary value problem corresponding to (1), where the position x is now in a bounded set $\mathcal{O}$ of boundary Γ.

At initial time $t = 0$, we set

$$f(t = 0, x, v) = f^0(x, v), \tag{21}$$

For points x on the boundary Γ, the distribution of incoming velocities (that is to say v such that $v \cdot n(x) < 0$, where $n(x)$ is the outer normal of Γ at x) must be specified. We consider one of the following three boundary condition (BC for short). The Dirichlet BC reads

$$f(t, x, v) = f_\Gamma(t, x, v), \qquad \forall x \in \Gamma, \quad \forall v \text{ s.t. } v \cdot n(x) < 0. \tag{22}$$

The reflecting BC is

$$f(t, x, v) = \int_{v' \cdot n(x) > 0} K(x, v, v') f(t, x, v') \, dv', \qquad \forall x \in \Gamma, \quad \forall v \text{ s.t. } v \cdot n(x) < 0, \tag{23}$$

where the kernel K is such that there is no normal mass flux across the boundary:

$$\int_\Omega v \cdot n(x) f(t, x, v) \, dv = 0, \tag{24}$$

and such that (23) is satisfied by the equilibrium E. The periodic BC can be used if the shape of $\mathcal{O}$ is symmetric: it reads

$$f(t, x, v) = f(t, Sx, v), \quad x \in \Gamma_1, \quad \forall v \tag{25}$$

7

where S is a one-to-one mapping from a part Γ_1 of Γ onto another part Γ_2.

Now we consider the corresponding initial and boundary conditions for the micro-macro formulation (15)–(16) of (1). In general, using the micro-macro decomposition into initial and boundary conditions (21)–(25) provides relations for $\rho + \varepsilon g$, but do not provides the values of ρ and g separately. Then it is easy to prove that the initial-boundary value problem for (15)–(16) is equivalent to the corresponding kinetic problem (1).

Here, we show that, in fact, all the initial and boundary conditions can be translated into separate conditions for ρ and g, except for the Dirichlet BC. The initial condition (21) gives

$$\rho(t = 0, x) = \left\langle f^0(x, .) \right\rangle \quad \text{and} \quad g(t = 0, x, v) = \frac{1}{\varepsilon}(f^0(x, v) - \left\langle f^0(x, .) \right\rangle). \qquad (26)$$

The reflecting BC (23) is satisfied by g only

$$g(t, x, v) = \int_{v' \cdot n(x) > 0} K(x, v, v') g(t, x, v') \, dv', \quad v \cdot n(x) < 0, \qquad (27)$$

while ρ is not prescribed, and the zero mass flux condition (24) gives

$$\int_\Omega v \cdot n(x) g(t, x, v) \, dv = 0. \qquad (28)$$

Since the periodic condition (25) holds for every v, g can be eliminated by integrating with respect to v to find that ρ is periodic, hence g is periodic too:

$$\rho(t, x) = \rho(t, Sx) \quad \text{and} \quad g(t, x, v) = g(t, Sx, v), \qquad x \in \Gamma_1. \qquad (29)$$

However, the Dirichlet BC relates the incoming part of $\rho + \varepsilon g$ to a given distribution f_Γ, then ρ and g cannot be separated: relation (22) only gives

$$\rho(t, x) + \varepsilon g(t, x, v) = f_\Gamma(t, x, v), \qquad \forall x \in \Gamma, \quad \forall v \text{ s.t. } v \cdot n(x) < 0. \qquad (30)$$

Finally, the initial and boundary conditions for the diffusion problem corresponding to these BC can be easily found by using the micro-macro formulation. As in section 2.3, g converges to $L^{-1}(vE) \cdot \nabla_x \rho_0$ and ρ converges to ρ_0 that satisfies (7). Moreover, if the initial condition f^0 is an equilibrium state $\rho^0 E$, then (26) gives the initial condition $\rho^0(t = 0, x) = \rho_0(x)$. If f^0 is not an equilibrium state, an initial layer problem should be solved, but we do not consider this problem here. For the reflecting BC, the zero mass flux condition (28) gives the following Neumann BC

$$(\kappa(x)\nabla_x \rho_0(t, x)) \cdot n(x) = 0. \qquad (31)$$

The periodic BC (29) gives a periodic condition for ρ_0. Finally, for the Dirichlet BC (22), if the boundary data is an equilibrium state $f_\Gamma(t, x, v) = \rho_\Gamma(t, x)E(v)$, then we get te limit Dirichlet BC

$$\rho_0(t, x) = \rho_\Gamma(t, x). \qquad (32)$$

8

At the contrary, if f_Γ is not an equilibrium state, then g cannot be bounded at the boundary. It contains a boundary layer term of the form $\frac{1}{\varepsilon}\phi(t, \frac{x}{\varepsilon}, v)$ which gives at the limit the following Dirichlet BC for ρ_0

$$\rho_0(t, x) = \rho_\Gamma(t, x) = \lim_{y \to +\infty} \chi(t, y, v), \tag{33}$$

where χ is the bounded solution of the following half-space (also called Milne) problem

$$\begin{aligned} v \cdot n(x) \partial_y \chi &= L\chi, \quad y > 0, \\ \chi(t, 0, v) &= f_\Gamma(t, x, v), \quad x \in \Gamma, \quad v \cdot n(x) > 0. \end{aligned} \tag{34}$$

Note that this limit is independent of v (see [2] for more details).

3 The numerical method

3.1 Semi-implicit time discretization

For discrete times $t_n = n\Delta t$ we consider approximations $\rho^n(x) \approx \rho(t_n, x)$ and $g^n(x, v) = g(t_n, x, v)$. In equation (16), the stiffest terms are the collision term Lg and the space derivative $v \cdot E\nabla_x \rho$. Our claim is that only the collision term has to be implicit to ensure the stability as ε goes to 0. All the other terms are explicit. Then the time discretization of (16) is

$$\frac{g^{n+1} - g^n}{\Delta t} + \frac{1}{\varepsilon}(I - \Pi)(v \cdot \nabla_x g^n) = \frac{1}{\varepsilon^2} Lg^{n+1} + \frac{1}{\varepsilon}(I - \Pi)S^n - \frac{1}{\varepsilon^2} v \cdot E\nabla_x \rho^n. \tag{35}$$

In the macroscopic equation (15), there is no stiff term, but to recover the correct diffusion limit, the flux of g is taken at time t_{n+1}, which gives

$$\frac{\rho^{n+1} - \rho^n}{\Delta t} + \nabla_x \cdot \langle vg^{n+1} \rangle = \langle S^n \rangle. \tag{36}$$

Note that as in the continuous case, it can be readily seen that g^{n+1} tends to $L^{-1}(vE) \cdot \nabla_x \rho^n$ as ε goes to zero, and hence passing to the limit in (36) leads to the following time explicit discretized version of the diffusion equation (7)

$$\frac{\rho^{n+1} - \rho^n}{\Delta t} + \nabla_x \cdot (\kappa \nabla_x \rho^n) = \langle S^n \rangle. \tag{37}$$

3.2 Fully discrete scheme

In this section, we restrict the presentation to the one-dimensional problem. We consider staggered grids defined by points $x_i = i\Delta x$ and $x_{i-\frac{1}{2}} = (i - \frac{1}{2})\Delta x$. Now the macroscopic density ρ is approximated at time t_n on the grid $\{x_i\}$ by values $\rho_i^n \approx \rho(t_n, x_i)$ while g is approximated on the grid $\{x_{i-\frac{1}{2}}\}$ by values $g_{i-\frac{1}{2}}^n(v) \approx g(t_n, x_{i-\frac{1}{2}}, v)$. The velocity variable is kept continuous here: see section 5 for a simple discretization.

9

Now since our goal is to get a numerical scheme that works uniformly for transport regimes ($\varepsilon = O(1)$) and diffusion regimes ($\varepsilon \ll 1$), we approximate the transport term $v\partial_x g^n$ in (35) by an upwind scheme, while the other space derivatives in (35) and (36) are approximated by centered differences. This gives

$$\frac{\rho_i^{n+1} - \rho_i^n}{\Delta t} + \left\langle v\frac{g_{i+\frac{1}{2}}^{n+1} - g_{i-\frac{1}{2}}^{n+1}}{\Delta x} \right\rangle = \langle S_i^n \rangle, \tag{38}$$

$$\frac{g_{i-\frac{1}{2}}^{n+1} - g_{i-\frac{1}{2}}^n}{\Delta t} + \frac{1}{\varepsilon\Delta x}(I - \Pi)\left(v^+(g_{i-\frac{1}{2}}^n - g_{i-\frac{3}{2}}^n) + v^-(g_{i+\frac{1}{2}}^n - g_{i-\frac{1}{2}}^n)\right) \tag{39}$$

$$= \frac{1}{\varepsilon^2}L_{i-\frac{1}{2}}g_{i-\frac{1}{2}}^{n+1} + \frac{1}{\varepsilon}(I - \Pi)S_{i-\frac{1}{2}}^n - \frac{1}{\varepsilon^2}vE\frac{\rho_i^n - \rho_{i-1}^n}{\Delta x},$$

where $v^\pm = \frac{v \pm |v|}{2}$. For an accurate description of transport regimes, higher order upwind approximations of $v\partial_x g$ can of course be considered, but this is not necessary in diffusive regimes.

3.3 Diffusion limit

For diffusion regimes, we assume that Δt can be taken independent of ε in scheme (38)–(39), a fact which holds true from the numerical simulations. See section 4 for a rigorous proof in a simple case. According to (39), we have

$$g_{i-\frac{1}{2}}^{n+1} = L_{i-\frac{1}{2}}^{-1}(vE)\frac{\rho_i^n - \rho_{i-1}^n}{\Delta x} + O(\varepsilon),$$

which implies that passing to the limit in (38) gives the following scheme

$$\frac{\rho_i^{n+1} - \rho_i^n}{\Delta t} + \frac{1}{\Delta x}\left(\kappa_{i+\frac{1}{2}}\frac{\rho_{i+1}^n - \rho_i^n}{\Delta x} - \kappa_{i-\frac{1}{2}}\frac{\rho_i^n - \rho_{i-1}^n}{\Delta x}\right) = \langle S_i^n \rangle, \tag{40}$$

where the diffusion coefficient is $\kappa_{i-\frac{1}{2}} = \left\langle vL_{i-\frac{1}{2}}^{-1}(vE) \right\rangle$. This is the classical three point explicit discretization of the diffusion equation (7).

Note that our scheme (38)–(39) involves the inversion of $I - \frac{\Delta t}{\varepsilon^2}L_{i-\frac{1}{2}}$. In the examples treated in section 5, this inversion is made exactly since L is diagonal. In a general case, this may be more difficult. But note that this problem is common to every AP scheme in the diffusion limit: they all require this kind of inversion. See [13] for a fast inversion technique by using Wild sums.

3.4 Numerical boundary conditions

It may be deduced from relations (38)–(39) that separated BC for ρ and g are necessary in our scheme. However, this is not completely true. Indeed, we consider the bounded space

10

domain $[0, 1]$ discretized by the bounded staggered grids $\{x_i = i\Delta x\}_{i=0}^N$ with $x_0 = 0$ and $x_N = 1$, and $\{x_{i-\frac{1}{2}} = (i - \frac{1}{2})\Delta x\}_{i=0}^{N+1}$ with $x_{-\frac{1}{2}} = -\frac{1}{2}\Delta x$ and $x_{N+\frac{1}{2}} = 1 + \frac{1}{2}\Delta x$. Now we assume that ρ and g are known at all grid points, at time t_n. Then we apply (39) to inner points only ($i = 1$ to N). Therefore this relation gives g^{n+1} at inner points and does not require any unknown value. Relation (38) is then applied to every point to obtain ρ_i^{n+1} for $i = 0$ to N. But for this we need outer values $g_{-\frac{1}{2}}^{n+1}$ and $g_{N+\frac{1}{2}}^{n+1}$ for **every** v, which is due to the use of centered differences in the macroscopic equation.

First, we explain how we determine these outer values, for *incoming* velocities. We discretize BC (30), (27) and (29) as follows. For Dirichlet BC, relation (30) is approximated by

$$
\begin{aligned}
\rho_0^{n+1} + \frac{\varepsilon}{2}(g_{-\frac{1}{2}}^{n+1}(v) + g_{\frac{1}{2}}^{n+1}(v)) = f_L(v), \qquad v > 0, \\
\rho_N^{n+1} + \frac{\varepsilon}{2}(g_{N-\frac{1}{2}}^{n+1}(v) + g_{N+\frac{1}{2}}^{n+1}(v)) = f_R(v), \qquad v < 0,
\end{aligned}
\tag{41}
$$

where f_L and f_R are the left and right data for incoming velocities. Reflecting boundary conditions (27) are approximated by the following relations between points $x_{-\frac{1}{2}}$ and $x_{\frac{1}{2}}$:

$$
\begin{aligned}
g_{-\frac{1}{2}}^{n+1}(v) = \int_{v'<0} K_0(v, v')g_{\frac{1}{2}}^{n+1}(v')\, dv', \quad v > 0, \\
g_{N+\frac{1}{2}}^{n+1}(v) = \int_{v'>0} K_N(v, v')g_{N-\frac{1}{2}}^{n+1}(v')\, dv', \quad v < 0,
\end{aligned}
\tag{42}
$$

which gives the following approximation of the zero mass flux relation (28)

$$
\left\langle v^+ g_{-\frac{1}{2}}^{n+1} + v^- g_{\frac{1}{2}}^{n+1} \right\rangle = 0,
\tag{43}
$$

and a similar relation at the right boundary. The periodic BC is approximated by the following relation between points $x_{-\frac{1}{2}}$ and $x_{N-\frac{1}{2}}$, and points $x_{N+\frac{1}{2}}$ and $x_{\frac{1}{2}}$

$$
g_{-\frac{1}{2}}^{n+1}(v) = g_{N-\frac{1}{2}}^{n+1}(v) \quad \text{and} \quad g_{N+\frac{1}{2}}^{n+1}(v) = g_{\frac{1}{2}}^{n+1}(v).
\tag{44}
$$

Now, we study the case of *outgoing* velocities. Note that relation (44) is valid for every v, while (41) and (42) are used only for incoming velocities. For Dirichlet or reflecting BC, we simply propose to use an artificial BC given by the following first order Neumann BC

$$
\begin{aligned}
g_{-\frac{1}{2}}^{n+1}(v) = g_{\frac{1}{2}}^{n+1}(v), \quad v < 0 \\
g_{N+\frac{1}{2}}^{n+1}(v) = g_{N-\frac{1}{2}}^{n+1}(v), \quad v > 0,
\end{aligned}
\tag{45}
$$

which is sufficient for most cases, while a second order Neumann BC is recommended in some cases (see section 5).

Now, we point out that relations (41), (42), (44) and (45) are not sufficient to obtain g^{n+1} at outer points: since ρ_0^{n+1} and ρ_N^{n+1} are not known, we also need to use relation (38)

for $i = 0$ and $i = N$ to determine all these boundary and outer values. It is only after this step that ρ_0^{n+1}, ρ_N^{n+1}, $g_{-\frac{1}{2}}^{n+1}$, and $g_{N+\frac{1}{2}}^{n+1}$ are fully determined. For clarity, we summarize below the different steps of our algorithm :

1. compute $g_{i-\frac{1}{2}}^{n+1}$ for $i = 1$ to N using (39);

2. compute ρ_i^{n+1} for $i = 1$ to $N - 1$ using (38);

3. eliminate $g_{-\frac{1}{2}}^{n+1}$, and $g_{N+\frac{1}{2}}^{n+1}$ into (38) for $i = 0$ and $i = N$ by using (41) and (45), or (42) and (45), or (44), and then compute ρ_0^{n+1} and ρ_N^{n+1};

4. use (41) and (45), or (42) and (45), or (44) to compute $g_{-\frac{1}{2}}^{n+1}$ and $g_{N+\frac{1}{2}}^{n+1}$.

Finally, we investigate the diffusion limit of our scheme when using these BC. For the inner values of ρ, we again obtain (40) but for i from 2 to $N - 1$ only. For boundary values ρ_0 and ρ_N, our analysis is the following. The relation satified by ρ_0^{n+1} for every ε is

$$\frac{\rho_0^{n+1} - \rho_0^n}{\Delta t} + \frac{1}{\Delta x}(\left\langle vg_{\frac{1}{2}}^{n+1}\right\rangle - \left\langle vg_{-\frac{1}{2}}^{n+1}\right\rangle) = \left\langle S_0^n\right\rangle,$$

where $\left\langle vg_{\frac{1}{2}}^{n+1}\right\rangle$ converges towards $\kappa_{\frac{1}{2}}\frac{1}{\Delta x}(\rho_1^n - \rho_0^n)$ as ε goes to 0.

For reflecting BC, the use of (42) and the artificial Neumann BC (45) for outgoing velocities gives $\left\langle vg_{-\frac{1}{2}}^{n+1}\right\rangle = 0$. Consequently the limiting relation satisfied by ρ_0^{n+1} can be written as

$$\frac{\rho_0^{n+1} - \rho_0^n}{\Delta t} + \frac{1}{\Delta x}\left(\kappa_{\frac{1}{2}}\frac{\rho_1^n - \rho_0^n}{\Delta x} - \kappa_{-\frac{1}{2}}\frac{\rho_0^n - \rho_{-1}^n}{\Delta x}\right) = \left\langle S_0^n\right\rangle,$$

where the fictious values ρ_{-1}^n and $\kappa_{-\frac{1}{2}}$ are defined as $\rho_{-1}^n = \rho_0^n$ and $\kappa_{-\frac{1}{2}} = \kappa_{\frac{1}{2}}$. This is indeed a first order approximation of the corresponding Neumann BC (31) for the diffusion problem. The same analysis can be made for the right BC.

For periodic BC, the use of (44) leads to the following limiting relations

$$\frac{\rho_0^{n+1} - \rho_0^n}{\Delta t} + \frac{1}{\Delta x}\left(\kappa_{\frac{1}{2}}\frac{\rho_1^n - \rho_0^n}{\Delta x} - \kappa_{N-\frac{1}{2}}\frac{\rho_N^n - \rho_{N-1}^n}{\Delta x}\right) = \left\langle S_0^n\right\rangle,$$

$$\frac{\rho_N^{n+1} - \rho_N^n}{\Delta t} + \frac{1}{\Delta x}\left(\kappa_{\frac{1}{2}}\frac{\rho_1^n - \rho_0^n}{\Delta x} - \kappa_{N-\frac{1}{2}}\frac{\rho_N^n - \rho_{N-1}^n}{\Delta x}\right) = \left\langle S_N^n\right\rangle.$$

If ρ^n and S^n are periodic, then we have $\rho_0^{n+1} = \rho_N^{n+1}$ which is the correct periodic BC for the diffusion equation, and hence ρ^{n+1} is periodic too.

Finally, for the Dirichlet BC, using (41) and (45) leads to the following relation for ρ_0

$$\frac{\rho_0^{n+1} - \rho_0^n}{\Delta t} + \frac{1}{\Delta x}\left(\left\langle vg_{\frac{1}{2}}^{n+1}\right\rangle - \left\langle v^+\left[\frac{2}{\varepsilon}(f_L - \rho_0^{n+1}) - g_{\frac{1}{2}}^{n+1}\right] + v^- g_{\frac{1}{2}}^{n+1}\right\rangle\right) = \left\langle S_0^n\right\rangle.$$

As ε goes to 0, the term in $O(\frac{1}{\varepsilon})$ does not explode since the relation is an implicit scheme for ρ_0^{n+1}. Instead, ρ_0^{n+1} converges to the value

$$\rho_0^{n+1} = \frac{\int_0^1 v f_L \, dv}{\int_0^1 v \, dv}. \tag{46}$$

If f_L is isotropic ($f_L = \rho_L$), then we get $\rho_0^{n+1} = \rho_L$ which is the correct Dirichlet BC for the diffusion equation. However, if f_L is not isotropic, (46) corresponds to an approximation of the half-space problem (34) by equalizing the half fluxes of χ at 0 and $+\infty$. This approximation is often used but could sometimes be insufficient in terms of accuracy. The same analysis can be made for the right boundary condition.

3.5 Comparison with other AP schemes

In this section, we discuss the main differences of our approach with other AP schemes.

In [18], Klar proposed a decomposition of f into $f_0 + \varepsilon f_1$, where f_0 and f_1 are solutions of the following coupled linear system:

$$\partial_t f_0 + v \partial_x f_1 = \frac{1}{\varepsilon^2} L f_0 + S$$
$$\partial_t f_1 + \frac{1}{\varepsilon^2} v \partial_x f_0 = \frac{1}{\varepsilon^2} L f_1.$$

Indeed, it is easy to check that $f_0 + \varepsilon f_1$ is a solution of (1). In the diffusive limit, f_0 is close to ρE and f_1 is close to the first order term of the Hilbert expansion. Consequently, this decomposition is very close to our micro-macro decomposition. The main difference lies in the evolution system for f_0 and f_1 which is very different from our system (15-16) for ρ and g. For instance, while our system couples the evolutions of the equilibrium part $f_0 = \rho E$ and the kinetic part $\varepsilon f_1 = f - f_0$, the two parts of the decomposition of [18] do not follow this mechanism during the time evolution. The equilibrium part has indeed to be extracted from both f_0 and f_1 at any time. Another difference lies in the numerical scheme itself: the stiffness of the equations is removed by using a time-splitting scheme between transport and collision, while no splitting is needed in our approach. The space discretization uses the same staggered grid strategy as we propose in this paper. More precisely, if $f_{0,i}^n$ is an approximation of $f_0(t_n, x_i, v)$ and $f_{1,i+\frac{1}{2}}^n$ is an approximation of $f_1(t_n, x_{i+\frac{1}{2}}, v)$, then these approximations are computed by the following scheme [18]:
transport steps:

$$\frac{f_{0,i}^{n+\frac{1}{2}} - f_{0,i}^n}{\Delta t} + v \frac{f_{1,i+\frac{1}{2}}^n - f_{1,i-\frac{1}{2}}^n}{\Delta x} = S_i^n,$$
$$f_{1,i+\frac{1}{2}}^{n+\frac{1}{2}} = f_{1,i+\frac{1}{2}}^n, \qquad \text{for } i = 0 \text{ to } N.$$

collision steps:

$$\frac{f_{0,i}^{n+1} - f_{0,i}^{n+\frac{1}{2}}}{\Delta t} = \frac{1}{\varepsilon^2} L f_{0,i}^{n+1}, \qquad \text{for } i = 0 \text{ to } N,$$

$$\frac{f_{1,i+\frac{1}{2}}^{n+1} - f_{1,i+\frac{1}{2}}^{n+\frac{1}{2}}}{\Delta t} = -\frac{1}{\varepsilon^2} v \frac{f_{0,i+1}^{n} - f_{0,i}^{n}}{\Delta x} + \frac{1}{\varepsilon^2} L f_{1,i+\frac{1}{2}}^{n+1}, \qquad \text{for } i = 0 \text{ to } N - 1.$$

At the boundaries, this scheme only requires to compute values $f_{1,-\frac{1}{2}}^{n+1}$ and $f_{1,N+\frac{1}{2}}^{n+1}$ for every v. We detail below only the case of the right boundary. The Dirichlet boundary condition is given by:

$$f_0 + \varepsilon f_1 = f_R, \ v < 0, \ x = 1, \qquad \text{and } f_0 - \varepsilon f_1 = q, \ v > 0, \ x = 1,$$

where q is an approximation of the outgoing solution of a Milne problem at the boundary given by $q = \frac{\int_{-1}^{0} v f_R \, dv}{v \, dv}$, so as to recover the correct boundary value in the diffusion regime. Numerically, this is translated into the following BC:

$$f_{1,N+\frac{1}{2}}^{n+1} = \begin{cases} \frac{2}{\varepsilon}(q - f_{0,N}^{n+1}) - f_{1,N-\frac{1}{2}}^{n+1}, & v > 0 \\ -\frac{2}{\varepsilon}(f_R - f_{0,N}^{n+1}) - f_{1,N-\frac{1}{2}}^{n+1}, & v < 0. \end{cases}$$

For a reflection BC, we use the asymptotic approximation $f_1(v) = f_1(-v)$ at $x = 1$ and the fact that f_1 should be even w.r.t v to get $f_1(v) = 0$, which is translated into $f_{1,N+\frac{1}{2}}^{n+1} = -f_{1,N-\frac{1}{2}}^{n+1}$. The periodic BC is obvious.

In [16], Jin, Pareschi and Toscani proposed another method based on the even-odd decomposition $f = r + \varepsilon j$, where $r = \frac{1}{2}(f(v) + f(-v))$ and $j = \frac{1}{2\varepsilon}(f(v) - f(-v))$. When ε is small, r is close to ρE, and j is close to the first order term of the Hilbert expansion. As for our micro-macro decomposition, it is easy to derive the following equivalent coupled system for r and j:

$$\partial_t r + v \partial_x j = \frac{1}{\varepsilon^2} L r + S$$

$$\partial_t j + \phi v \partial_x r = \frac{1}{\varepsilon^2} (L j - (1 - \phi) v \partial_x r),$$

where $\phi = \min(1, \frac{1}{\varepsilon})$ is defined so as to make the left hand-side a strictly hyperbolic system. This system is very close to the system of Klar (see the case $\phi = 1$), and hence to our system also, but it is discretized differently. According to [16], the numerical approximation of this system is based on a second order time splitting between convection and relaxtation, coupled to a semi-implicit discretization of the relaxation step, and a TVD second order scheme for the convection step. In our comparisons, we shall only use a first order time splitting scheme,

which writes for $i = 1$ to N:

transport step:

$$r_i^{n+\frac{1}{2}} = r_i^n - \frac{\Delta t}{2\Delta x \phi} v(j_{i+1}^n - j_{i-1}^n) + \frac{\Delta t}{2\Delta x} v(r_{i+1}^n - 2r_i^n + r_{i-1}^n)$$

$$- \frac{\Delta t}{2\Delta x} \frac{1}{2}(1 - \frac{\Delta t}{\Delta x} v)(A_i - A_{i-1} + B_{i+1} - B_i),$$

$$j_i^{n+\frac{1}{2}} = j_i^n - \frac{\Delta t}{2\Delta x \phi} v(r_{i+1}^n - r_{i-1}^n) + \frac{\Delta t}{2\Delta x} v(r_{i+1}^n - 2r_i^n + r_{i-1}^n)$$

$$- \frac{\Delta t \sqrt{\phi}}{2\Delta x} \frac{1}{2}(1 - \frac{\Delta t}{\Delta x} v)(A_i - A_{i-1} - B_{i+1} + B_i),$$

relaxation step:

$$r_i^{n+1} = \frac{1}{1 + \frac{\Delta t}{\varepsilon^2}} \left(r_i^{n+\frac{1}{2}} + \frac{\Delta t}{\varepsilon^2} \rho_i^{n+\frac{1}{2}} \right),$$

$$j_i^{n+1} = \frac{1}{1 + \frac{\Delta t}{\varepsilon^2}} \left(j_i^{n+\frac{1}{2}} - \frac{\Delta t}{\varepsilon^2} (1 - \varepsilon^2 \phi) \frac{1}{2\Delta x} v \left(r_{i+1}^{n+\frac{1}{2}} - r_{i-1}^{n+\frac{1}{2}} \right) \right),$$

where $r_i^n(v) \approx r(t_n, x_i, v)$ and the same for j. Coefficients A_i and B_i are slope limiters. This scheme needs the numerical boundary values r_0^n, r_{N+1}^n, j_0^n, j_{N+1}^n. At the right boundary, for Dirichlet BC, it is proposed in [16] to use the relation $(r + \varepsilon j)(1, v < 0) = f_R$ and the asymptotic relation $j = -v\partial_x r$ to get the following numerical BC:

$$r_{N+1}^n = \frac{1}{\frac{1}{2} + \varepsilon \frac{v}{\Delta x}} \left(f_R - \left(\frac{1}{2} - \frac{\varepsilon v}{\Delta x} \right) r_N^n \right) \quad \text{and} \quad j_{N+1}^n = -j_N^n - 2v \frac{r_{N+1}^n - r_N^n}{\Delta x}.$$

For a reflection BC, we use in this paper the even parity of j and again the asymptotic relation $j = -v\partial_x r$ to get the following approximation: $j_{N+1}^n = j_N^n$ and $r_{N+1}^n = r_N^n$. The periodic BC is obvious.

To summarize, we note that these methods as well as our approach are based on a very similar idea: a decomposition of f into a main part that is close to the equilibrium in diffusive regimes, and another part that vanishes in this limit. The main differences are: the main part of the decomposition is macroscopic only in our method (which is more economic for multi-dimensional computations), the coupled system used for the micro and macro parts are rather different, and the numerical schemes designed to discretize this system as well.

There is also another approach to obtain AP schemes, proposed by Gosse and Toscani in [8, 9], which is very different from our method (and even from the methods by Klar or Pareschi-Toscani-Jin). They do not use any decomposition of f, but instead the theory of "well balanced schemes", in which the steady solution is used to compute intermediate states into a Godunov like-solver that takes the collision term into account. This technique has been proved by the authors to be efficient for the telegraph equation and also for the linear transport equation. An important point of this approach is that it leads to strong mathematical results (uniform stability and convergence).

4 Stability analysis

In this section we prove the uniform stability of our scheme (39)–(38) with respect to ε, for the simple case of the telegraph equation (5). Scheme (39)–(38) is applied to the micro-macro formulation (20) to obtain

$$\frac{\alpha_{i+\frac{1}{2}}^{n+1} - \alpha_{i+\frac{1}{2}}^n}{\Delta t} + \frac{1}{\varepsilon \Delta x}\left[(\alpha_{i+\frac{1}{2}}^n - \alpha_{i-\frac{1}{2}}^n) - \frac{1}{2}(\alpha_{i+\frac{1}{2}}^n - \alpha_{i-\frac{1}{2}}^n - \beta_{i+\frac{3}{2}}^n + \beta_{i+\frac{1}{2}}^n)\right] \tag{47}$$

$$= -\frac{1}{\varepsilon^2}\alpha_{i+\frac{1}{2}}^{n+1} - \frac{1}{\varepsilon^2}\frac{\rho_{i+1}^n - \rho_i^n}{\Delta x},$$

$$\frac{\beta_{i+\frac{1}{2}}^{n+1} - \beta_{i+\frac{1}{2}}^n}{\Delta t} + \frac{1}{\varepsilon \Delta x}\left[-(\beta_{i+\frac{3}{2}}^n - \beta_{i+\frac{1}{2}}^n) - \frac{1}{2}(\alpha_{i+\frac{1}{2}}^n - \alpha_{i-\frac{1}{2}}^n - \beta_{i+\frac{3}{2}}^n + \beta_{i+\frac{1}{2}}^n)\right] \tag{48}$$

$$= -\frac{1}{\varepsilon^2}\beta_{i+\frac{1}{2}}^{n+1} + \frac{1}{\varepsilon^2}\frac{\rho_{i+1}^n - \rho_i^n}{\Delta x},$$

$$\frac{\rho_i^{n+1} - \rho_i^n}{\Delta t} + \frac{1}{2\Delta x}\left[(\alpha_{i+\frac{1}{2}}^{n+1} - \beta_{i+\frac{1}{2}}^{n+1}) - (\alpha_{i-\frac{1}{2}}^{n+1} - \beta_{i-\frac{1}{2}}^{n+1})\right] = 0.$$

However, this scheme can be put in a much simpler form by using the flux variable $j = \frac{1}{2\varepsilon}(u - v) = \frac{1}{2}(\alpha - \beta)$. Therefore, substracting (48) to (47) and using the fact that $\alpha_{i+\frac{1}{2}}^n = -\beta_{i+\frac{1}{2}}^n$ for every i, we get the equivalent scheme

$$\frac{\rho_i^{n+1} - \rho_i^n}{\Delta t} + \frac{1}{\Delta x}(j_{i+\frac{1}{2}}^{n+1} - j_{i-\frac{1}{2}}^{n+1}) = 0, \tag{49}$$

$$\frac{j_{i+\frac{1}{2}}^{n+1} - j_{i+\frac{1}{2}}^n}{\Delta t} - \frac{1}{2\varepsilon \Delta x}(j_{i+\frac{3}{2}}^n - 2j_{i+\frac{1}{2}}^n + j_{i-\frac{1}{2}}^n) = -\frac{1}{\varepsilon^2}j_{i+\frac{1}{2}}^{n+1} - \frac{1}{\varepsilon^2}\frac{\rho_{i+1}^n - \rho_i^n}{\Delta x}, \tag{50}$$

which is clearly a discretization of the form (6) of the telegraph equation. Note the numerical diffusion term in (50): as explained in section 3.2, this diffusion can be reduced by using a second order extension of the upwind approximation of the transport terms $\partial_x \alpha$ and $\partial_x \beta$. As stated in section 3.3, this scheme gives in the limit $\varepsilon = 0$ the following classical explicit discretization of the linear heat equation

$$\frac{\rho_i^{n+1} - \rho_i^n}{\Delta t} - \frac{1}{\Delta x^2}\left(\rho_{i+1}^n - 2\rho_i^n + \rho_{i-1}^n\right) = 0. \tag{51}$$

Now we prove the following stability theorem.

Theorem 4.1. *The scheme (49–50) is l^2-stable, i.e. we have*

$$\sum_i (\rho_i^n)^2 + (\varepsilon j_{i+\frac{1}{2}}^n)^2 \le \sum_i (\rho^0 i)^2 + (\varepsilon j_{i+\frac{1}{2}}^0)^2$$

for every n, if Δt satisfies the following condition

$$\Delta t \le \frac{1}{2}\left(\frac{\Delta x^2}{2} + \varepsilon \Delta x\right). \tag{52}$$

Note that the CFL condition (52) can be viewed as an average of the diffusive CFL condition $\Delta t \leq \frac{1}{2}\Delta x^2$ (needed for the diffusion scheme (51)) and of the convection CFL constraint $\Delta t \leq \varepsilon \Delta x$. It shows that the scheme is l^2-stable uniformly in ε, that is to say the diffusive CFL condition $\Delta t \leq \frac{1}{4}\Delta x^2$ is sufficient for stability for small ε, while half of the convection CFL is sufficient for $\varepsilon = O(1)$.

Now we give a proof of this theorem which is based on a standard Von Neumann analysis.

Proof. We introduce the following notations $J^n_{i+\frac{1}{2}} = \varepsilon j^n_{i+\frac{1}{2}}$, $\sigma = \frac{\Delta t}{\varepsilon \Delta x}$, and $\lambda = \frac{1}{1+\Delta t/\varepsilon^2}$. Then the scheme (49)–(50) reads

$$
\begin{aligned}
\rho^{n+1}_j &= \rho^n_j - \sigma(J^{n+1}_{j+\frac{1}{2}} - J^{n+1}_{j-\frac{1}{2}}), \\
J^{n+1}_{j+\frac{1}{2}} &= \lambda\left(J^n_{j+\frac{1}{2}} + \frac{\sigma}{2}(J^n_{j+\frac{3}{2}} - 2J^n_{j+\frac{1}{2}} + J^n_{j-\frac{1}{2}}) - \sigma(\rho^n_{j+1} - \rho^n_j)\right),
\end{aligned}
\tag{53}
$$

where the index i has been replaced by j to avoid confusion with $i = \sqrt{-1}$. Taking ρ^n_j and $J^n_{j+\frac{1}{2}}$ on the form of elementary waves $\rho^n_j = \rho^n(\xi)e^{ij\xi}$ and $J^n_{j+\frac{1}{2}} = J^n(\xi)e^{i(j+\frac{1}{2})\xi}$, we find the following relations on the amplitudes

$$
\begin{aligned}
\rho^{n+1} &= \rho^n - i2\sigma\sin\theta J^{n+1}, \\
J^{n+1} &= \lambda\left((1 - 2\sigma\sin^2\theta)J^n - i2\sigma\sin\theta\rho^n\right)
\end{aligned}
$$

where $\theta = \frac{\xi}{2}$. This can be written under a matrix form

$$
\begin{pmatrix} \rho^{n+1} \\ J^{n+1} \end{pmatrix} = A \begin{pmatrix} \rho^n \\ J^n \end{pmatrix}, \quad \text{with} \quad A = \begin{pmatrix} 1 - 4\sigma^2\lambda\sin^2\theta & -i(1 - 2\sigma\sin^2\theta)2\sigma\lambda\sin\theta \\ -i2\sigma\lambda\sin\theta & (1 - 2\sigma\sin^2\theta)\lambda \end{pmatrix}.
$$

Consequently, to prove the theorem, it is sufficient to prove that $\|A\|_2 \leq 1$ under the CFL condition (52). Here we denote by $\|A\|_2$ the matrix 2-norm induced by the Euclidean norm in $\mathbb{R}^2$. Note that $\|A\|_2^2$ is the largest eigenvalue of A^*A. Then we denote by T and D the trace and determinant of A^*A. Since the eigenvalues of A^*A are non-negative, it is easy to see that the maximum eigenvalue is $T + \sqrt{T^2 - 4D}$, which must be lower than 1 to ensure the stability of our scheme. This translates to $2 - 2T + 4D \geq 0$, and after explicit calculations of T and D gives

$$
4\sigma^2\lambda\sin^4\theta + 4\sigma\lambda(\sigma - 1)\sin^2\theta + 2(\lambda - 1) \leq 0.
$$

It is not difficult to see that this inequality is satisfied for every θ if and only if it is satisfied for $\sin^2\theta = 0$ or 1. The first condition is true since $\lambda \leq 1$, and the second one is true if $4\sigma^2\lambda + 4\sigma\lambda(\sigma - 1) + 2(\lambda - 1) \leq 0$. Using the definition of λ and σ in this relation directly gives the CFL condition (52). $\qquad\square$

We believe that an extension of this L^2-stability result for general linear kinetic equations could be obtained. Indeed, such a proof has been given in [24] by Klar and Unterreiter for the scheme proposed by Klar [19], which is quite close to ours. This question will be investigated into details in a forthcoming work.

5 Numerical tests

5.1 Telegraph equation

We compare the results obtained with our AP micro-macro scheme (49)–(50) (referred to as LM) to the results obtained with a standard explicit discretization of the original equation (5) written in kinetic variables (for large ε) and to the results obtained with the explicit discretization (40) of the diffusion limit (for small ε). We also compare our scheme to the AP schemes proposed in [19] (denoted by K) and in [15] (denoted by JPT).

The space domain is $[-1, 1]$ discretized with 100 points. We use periodic boundary conditions, and the initial data is the isotropic data $u = v = \rho$ defined by the following square-shaped function $\rho(x) = 1$ for $x \in [-0.2, 0.2]$ and 0 elsewhere. For our scheme, the time step is chosen according to the CFL condition (52), while the explicit scheme and diffusive scheme require $\Delta t \leq (\frac{1}{2\varepsilon} + \frac{1}{\Delta x})^{-1}$ and $\Delta t \leq \frac{\Delta x^2}{2}$, respectively.

First we show in figures 1 and 2 a comparison of ρ for $\varepsilon = 1$ at different times $t = 1/10$, $2/10$, $3/10$, $5/10$ between our scheme LM and the explicit scheme. We see that the scheme LM correctly describes the solution at any time, even if it is a little bit more diffusive than the explicit scheme. For a fair comparison, we also show the results obtained with schemes K and JPT in figure 3 at time $t = 3/10$. It is clearly seen that K is very oscillating (top), which is due to the lack of numerical viscosity in the transport terms, while JPT is more accurate than our scheme LM (bottom).

For small ε regime, we show in figures 4 and 5 a comparison for $\varepsilon = 10^{-10}$ at different times $t = \varepsilon/100$, $2\varepsilon/10$, $3\varepsilon/10$, $5\varepsilon/10$ between our scheme LM and the diffusion scheme. We see that our scheme LM gives a solution which is very close to the diffusion solution at any time. We also show the results obtained with schemes K and JPT in figures 6 and 7 at times $t = \varepsilon/100, 3\varepsilon/10$. Now K is also very accurate, while for JPT, at the shortest time, one can observe very slight oscillations in the stiff parts of the curve. This is due to the diffusion limit scheme of JPT that uses the two-step stencil $i - 2, i, i + 2$ (see [16]): this is not an accurate scheme for a solution that has sharp gradients like in this test case for short times.

5.2 One-group transport equation in slab geometry

Here we make the same kind of study for our AP micro-macro scheme (38)–(39) (denoted by LM) applied to equation (4), or more precisely to (18)–(19) in the micro-macro formulation. Depending on the regime, we compare this scheme to a standard explicit discretization of (4) or to the explicit discretization of the diffusion limit (7). For the explicit scheme, the results are obtained after a mesh convergence study: the number of points is sufficiently large to consider that the scheme has converged to the exact solution. Contrary to what is sometimes done in the literature, we believe that this validation is more reliable than considering the AP scheme with a large number of points as the reference solution (this last approach is rather adapted to a convergence study).

Our method is also compared to schemes K [19] and JPT [15] mentioned in the previous section. Note that here, all the upwind discretizations used in schemes LM and JPT are

second order in space.

For our comparison, we use several examples (1 to 6) taken in [19] and [15]. In all these test cases, Dirichlet boundary conditions are used. The velocity set is the standard 16-points Gaussian quadrature set in $[-1, 1]$. By analogy with the CFL condition (52) stated for the telegraph equation, the CFL used for our scheme LM is here

$$\Delta t \leq \frac{1}{2} \min \left(\frac{\Delta x^2}{2 \frac{1}{3 \sigma_S}} + \varepsilon \Delta x \right).$$

An additional test case (example 7) is used to investigate a reflection boundary condition. Every curves show the profile of the density ρ.

Example 1 Kinetic regime with isotropic boundary conditions:

$$x \in [0, 1], \qquad f_L(v) = 0, \qquad f_R(v) = 1,$$
$$\sigma_S = 1, \qquad \sigma_A = 0, \qquad G = 0, \qquad \varepsilon = 1.$$

The results are plotted at times $t = 0.1$, 0.4, 1.0, 1.6, and 4. The AP schemes LM, K and JPT use 25 and 200 points. The explicit scheme uses 1000 points. In figure 8, we observe that our scheme LM is very close to the reference solution, except with the coarse discretization for short times $t = 0.1$ and $t = 0.4$. In these cases, the results are not very accurate at the right boundary and in front of the incoming profile. In figure 9, we see that scheme JPT behaves similarly. At the contrary, in figure 10 scheme K seems more accurate with the coarse discretization, but it is quite oscillating with the thinest grid, except fot the large time $t = 4$.

Example 2 Diffusion regime with isotropic boundary conditions:

$$x \in [0, 1], \qquad f_L(v) = 1, \qquad f_R(v) = 0,$$
$$\sigma_S = 1, \qquad \sigma_A = 0, \qquad G = 0, \qquad \varepsilon = 10^{-8}.$$

The results are plotted at times $t = 0.01$, 0.05, 0.15 and 2. The AP schemes LM and JPT use 25 and 200 points. The diffusion scheme uses 200 points. In figure 11, we see that schemes LM and JPT are very close to the reference solution at any times for both coarse and fine discretizations. Note that here, scheme K is not used, since we observed that the numerical boundary conditions proposed in [19] produce stiff terms that require prohibitively small time steps when ε is small. However, we believe that this could easily be fixed by using implicit boundary conditions as in our scheme LM. Namely, inverting steps 1 and 2 of [19] (see p. 1081 of this reference) should be sufficient to ensure uniform stability. See also another kind of implicit boundary conditions in [22].

Example 3 Intermediate regime with isotropic boundary conditions, variable scattering frequency, and source term:

$$x \in [0, 1], \qquad f_L(v) = 0, \qquad f_R(v) = 0,$$
$$\sigma_S = 1 + (10x)^2, \qquad \sigma_A = 0, \qquad G = 1, \qquad \varepsilon = 10^{-2}.$$

The results are plotted at times $t = 0.4$ with 40 and 200 points in figure 12. The reference solution is obtained with the explicit scheme using 20 000 points. We observe that all the schemes provide results that are very close to the reference solution.

Example 4 Intermediate regime with non-isotropic boundary conditions that generate a boundary layer:

$$x \in [0, 1], \qquad f_L(v) = v, \qquad f_R(v) = 0,$$
$$\sigma_S = 1, \qquad \sigma_A = 0, \qquad G = 0, \qquad \varepsilon = 10^{-2}.$$

The results are plotted at times $t = 0.4$ with 25 and 200 points in figure 13. The reference solution is obtained with the explicit scheme using 20 000 points. We also consider the diffusion scheme with 25 points, with a left boundary condition $\rho_L = 17/24$ computed by formula (14) given in [19]. With the coarse discretization, the boundary layer is not resolved, but we observe that all the schemes are close to the reference solution inside the domain (far from the boundary). With the fine discretization, the boundary layer is resolved: again all the schemes are close to the reference solution, even inside the boundary layer. However, K seems to be a little bit more accurate than LM and JPT.

Example 5 Same case as in the previous example, but in a more diffusive regime, since $\varepsilon = 10^{-4}$ (see figure 14). In this case, using the explicit scheme is prohibitively expensive, and the reference solution outside the boundary layer is given by the diffusion scheme. Here the boundary layer is not resolved by any scheme, even with the fine discretization. It can be seen that our LM scheme and the JPT scheme are very close, but do not accurately capture the solution inside the domain. For LM scheme, this is due to the fact that the boundary value of the density produced by this scheme is not correct (as explained at the end of section 3.4). Note that even scheme K is not very accurate inside the domain, while it is designed to be very accurate at the boundary.

Example 6 This is a two-material problem used in [25, 19, 15], at stationary time. Here we also compare the results for a short time. The parameters are the following

$$x \in [0, 11], \qquad f_L(v) = 5, \qquad f_R(v) = 0,$$
$$\sigma_S = 0, \qquad \sigma_A = 1, \qquad G = 0 \qquad \text{for } x \in [0, 1],$$
$$\sigma_S = 100, \qquad \sigma_A = 0, \qquad G = 0 \qquad \text{for } x \in]1, 11].$$

Following [25], the parameter ε is set to 1, which means that non-rescaled variables are used here. Due to the scattering coefficient, the diffusion regime is obtained for long times in the domain $]1, 11]$ (this correspond to a value $\varepsilon = 0.01$ in the rescaled formulation). An interface layer is produced between the purely absorbing region $[0, 1]$ and the scattering domain $[1, 11]$. We compare the different schemes at an unsteady time $t = 2000$ (figure 15), and at steady state reached at $t = 20000$ (figure 16). Two meshes are used: a coarse one ($\Delta x = 0.05$ in $[0, 1]$ and $\Delta x = 1$ in $[1, 11]$), and a 5 times as thin mesh ($\Delta x = 0.01$ in $[0, 1]$ and $\Delta x = 0.2$ in $[1, 11]$). The reference solution is obtained with the explicit scheme using 22 000 points. We observe that for the unsteady time (figure 15), schemes LM and K are very close to the reference solution, except at the interface where slight differences can be seen. At the contrary, scheme JPT is not accurate in the scattering region. This is probably due to the fact that it uses a boundary condition that is correct only in diffusive regime (long times) or at steady state. There is no large differences between the two meshes. For the steady state (figure 16) all the schemes are close to the reference solution, but our scheme LM seems the most accurate with the thin mesh.

Example 7 This last test is designed to investigate the behavior of our scheme in case of a specular reflection boundary condition:

$$x \in [0, 1], \qquad f_L(v) = 1, \qquad f_R(v) = f_R(-v),$$
$$\sigma_S = 1, \qquad \sigma_A = 0, \qquad G = 0.$$

The results are plotted at times $t = 2$ with 20 and 200 points in figures 17 and 18 for four different regimes: $\varepsilon = 1, 10^{-1}, 10^{-2}$ and 10^{-10}. Here, the artificial boundary condition for outgoing velocities needed by our scheme LM is a second order Neumann condition: this gives much more accurate results that the first order condition. We mention that the reflection boundary condition has not been studied in [19, 16]. Therefore, in this test, we have developed suitable numerical boundary conditions for schemes JPT and K. However, we are note sure that they are the most relevant numerical BC for these schemes.

For the regimes $\varepsilon = 1, 10^{-1}, 10^{-2}$, the reference solution is obtained with the explicit scheme with 200, 1000, and 10 000 points, respectively. For the diffusive regime $\varepsilon = 10^{-10}$ the reference solution is the converged result obtained by the diffusion scheme with 200 points.

For the kinetic regime (top of figure 17), our scheme LM seems to be the most accurate with the coarse discretization, while JPT is less accurate at the right boundary. With the thin discretization, LM and JPT are very close to the reference solution, while K is oscillating (as noted in example 1). For the regime $\varepsilon = 0.1$ (bottom of figure 17), all the schemes are very close for both discretizations. For the intermediate and diffusion regimes ($\varepsilon = 0.01$ and 10^{-10}, see figure 18), all the schemes are very close to the reference solution. As in example 2, K is not used for $\varepsilon = 10^{-10}$.

6 Conclusion

We have presented a new method to design AP schemes for unstationary linear transport equations. This method is based on a very general micro-macro decomposition of the distribution function, a projection technique to obtain a coupled system of two evolution equations for the microscopic and macroscopic components, and a suitable semi-implicit time discretization. When applied to the simple telegraph model, this method has been proved to be uniformly stable with respect to the mean free path.

As compared to the method K of [19] and JPT of [16], our method generally behaves similarly, but we observed the following differences:

- for kinetic regimes ($\varepsilon = O(1)$):

  - it is more diffusive than JPT for non-smooth solutions, but does not generate oscillation as opposed to K;

  - the artificial boundary condition for outgoing velocities in case of Dirichlet BC is less accurate than K.

- for diffusive regimes ($\varepsilon \ll 1$):

  - when there is no boundary layer, our method is very accurate at any time, and even more accurate than JPT for short times in case of non-regular solutions;

  - in case of (under-resolved) boundary layers: our approach is not very accurate as compared to the diffusion equation inside the domain, but schemes K and JPT do not seem more accurate.

In our opinion, the main advantage of this method is its generality: indeed it can also be applied to other kinetic equations with different scalings (diffusion and hydrodynamic scalings). Of course, it could be easily applied to the linear Boltzmann equation of semi-conductors, but it has already been applied to the nonlinear Boltzmann equation of rarefied gas dynamics in [3] to obtain a numerical method that preserves the compressible Navier-Stokes asymptotics.

Natural perspectives are: find more suitable boundary conditions for a more accurate solution of boundary layer problems; extension to multidimensional case, which should be a straightforward adaptation of the present strategy; the extension of our approach to the low Mach number asymptotics of the Boltzmann equation; rigorous proof of the uniform stability of our method in a general linear case, in the spirit of [24] for instance.

References

[1] G. Bal and Y. Maday. Coupling of transport and diffusion models in linear transport theory. *M2AN Math. Model. Numer. Anal.*, 36(1):69–86, 2002.

[2] C. Bardos, R. Santos, and R. Sentis. Diffusion approximation and computation of the critical size. *Trans. Amer. Math. Soc.*, 284(2):617–649, 1984.

[3] M. Bennoune, M. Lemou, and L. Mieussens. Uniformly stable numerical schemes for the Bolztmann equation preserving compressible Navier-Stokes asympotics. To appear in the Journal of Computational Physics.

[4] P. Degond and S. Jin. A smooth transition model between kinetic and diffusion equations. *SIAM J. Numer. Anal.*, 42(6):2671–2687 (electronic), 2005.

[5] P. Degond, J.-G. Liu, and L. Mieussens. Macroscopic fluid models with localized kinetic upscaling effects. *Multiscale Modeling & Simulation*, 5(3):940–979, 2006.

[6] P. Degond and C. Schmeiser. Kinetic boundary layers and fluid-kinetic coupling in semiconductors. *Transport Theory Statist. Phys.*, 28(1):31–55, 1999.

[7] F. Golse, S. Jin, and C. D. Levermore. A domain decomposition analysis for a two-scale linear transport problem. *M2AN Math. Model. Numer. Anal.*, 37(6):869–892, 2003.

[8] L. Gosse and G. Toscani. An asymptotic-preserving well-balanced scheme for the hyperbolic heat equations. *C. R. Math. Acad. Sci. Paris*, 334(4):337–342, 2002.

[9] L. Gosse and G. Toscani. Asymptotic-preserving & well-balanced schemes for radiative transfer and the Rosseland approximation. *Numer. Math.*, 98(2):223–250, 2004.

[10] S. Jin. Efficient asymptotic-preserving (AP) schemes for some multiscale kinetic equations. *SIAM J. Sci. Comput.*, 21(2):441–454 (electronic), 1999.

[11] S. Jin and C. D. Levermore. The discrete-ordinate method in diffusive regimes. *Transport Theory Statist. Phys.*, 20(5-6):413–439, 1991.

[12] S. Jin and C. D. Levermore. Fully discrete numerical transfer in diffusive regimes. *Transport Theory Statist. Phys.*, 22(6):739–791, 1993.

[13] S. Jin and L. Pareschi. Discretization of the multiscale semiconductor Boltzmann equation by diffusive relaxation schemes. *J. Comput. Phys.*, 161(1):312–330, 2000.

[14] S. Jin and L. Pareschi. Asymptotic-preserving (AP) schemes for multiscale kinetic equations: a unified approach. In *Hyperbolic problems: theory, numerics, applications, Vol. I, II (Magdeburg, 2000)*, volume 141 of *Internat. Ser. Numer. Math., 140*, pages 573–582. Birkhäuser, Basel, 2001.

[15] S. Jin, L. Pareschi, and G. Toscani. Diffusive relaxation schemes for multiscale discrete-velocity kinetic equations. *SIAM J. Numer. Anal.*, 35(6):2405–2439 (electronic), 1998.

[16] S. Jin, L. Pareschi, and G. Toscani. Uniformly accurate diffusive relaxation schemes for multiscale transport equations. *SIAM J. Numer. Anal.*, 38(3):913–936 (electronic), 2000.

[17] S. Jin and Z. P. Xin. The relaxation schemes for systems of conservation laws in arbitrary space dimensions. *Comm. Pure Appl. Math.*, 48(3):235–276, 1995.

[18] A. Klar. Asymptotic-induced domain decomposition methods for kinetic and drift diffusion semiconductor equations. *SIAM J. Sci. Comput.*, 19(6):2032–2050 (electronic), 1998.

[19] A. Klar. An asymptotic-induced scheme for nonstationary transport equations in the diffusive limit. *SIAM J. Numer. Anal.*, 35(3):1073–1094 (electronic), 1998.

[20] A. Klar. An asymptotic preserving numerical scheme for kinetic equations in the low Mach number limit. *SIAM J. Numer. Anal.*, 36(5):1507–1527 (electronic), 1999.

[21] A. Klar. A numerical method for kinetic semiconductor equations in the drift-diffusion limit. *SIAM J. Sci. Comput.*, 20(5):1696–1712 (electronic), 1999.

[22] A. Klar and C. Schmeiser. Numerical passage from radiative heat transfer to nonlinear diffusion models. *Math. Models Methods Appl. Sci.*, 11(5):749–767, 2001.

[23] A. Klar and N. Siedow. Boundary layers and domain decomposition for radiative heat transfer and diffusion equations: applications to glass manufacturing process. *European J. Appl. Math.*, 9(4):351–372, 1998.

[24] A. Klar and A. Unterreiter. Uniform stability of a finite difference scheme for transport equations in diffusive regimes. *SIAM J. Numer. Anal.*, 40(3):891–913 (electronic), 2002.

[25] A. W. Larsen and J. E. Morel. Asymptotic solutions of numerical transport problems in optically thick, diffusive regimes. II. *J. Comput. Phys.*, 83(1):212–236, 1989.

[26] A. W. Larsen, J. E. Morel, and W. F. Miller Jr. Asymptotic solutions of numerical transport problems in optically thick, diffusive regimes. *J. Comput. Phys.*, 69(2):283–324, 1987.

[27] G. Naldi and L. Pareschi. Numerical schemes for kinetic equations in diffusive regimes. *Appl. Math. Lett.*, 11(2):29–35, 1998.
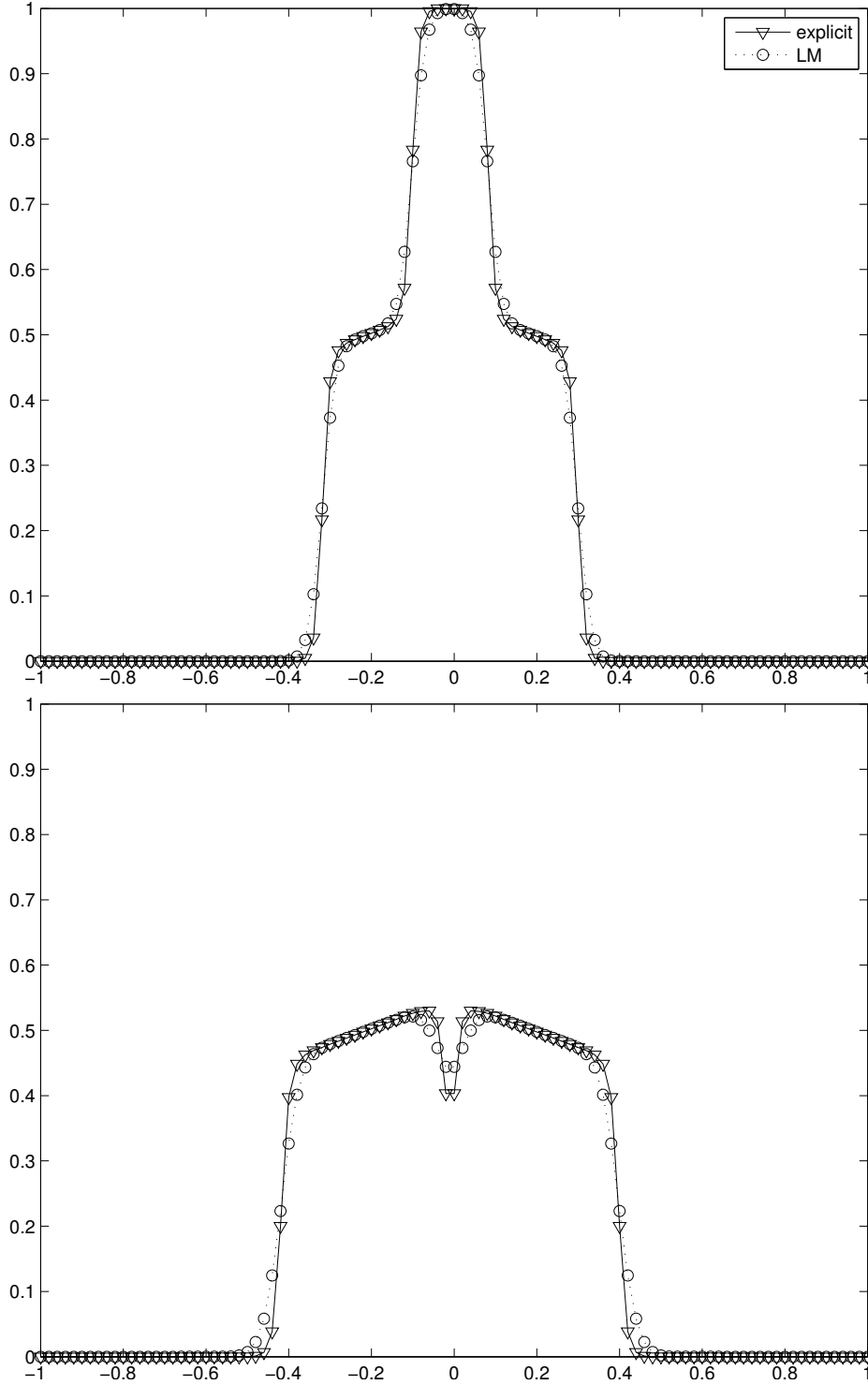
Figure 1: Telegraph equation $\varepsilon = 1$: comparison between explicit and LM schemes: $t = 1/10$ (top), $t = 2/10$ (bottom).
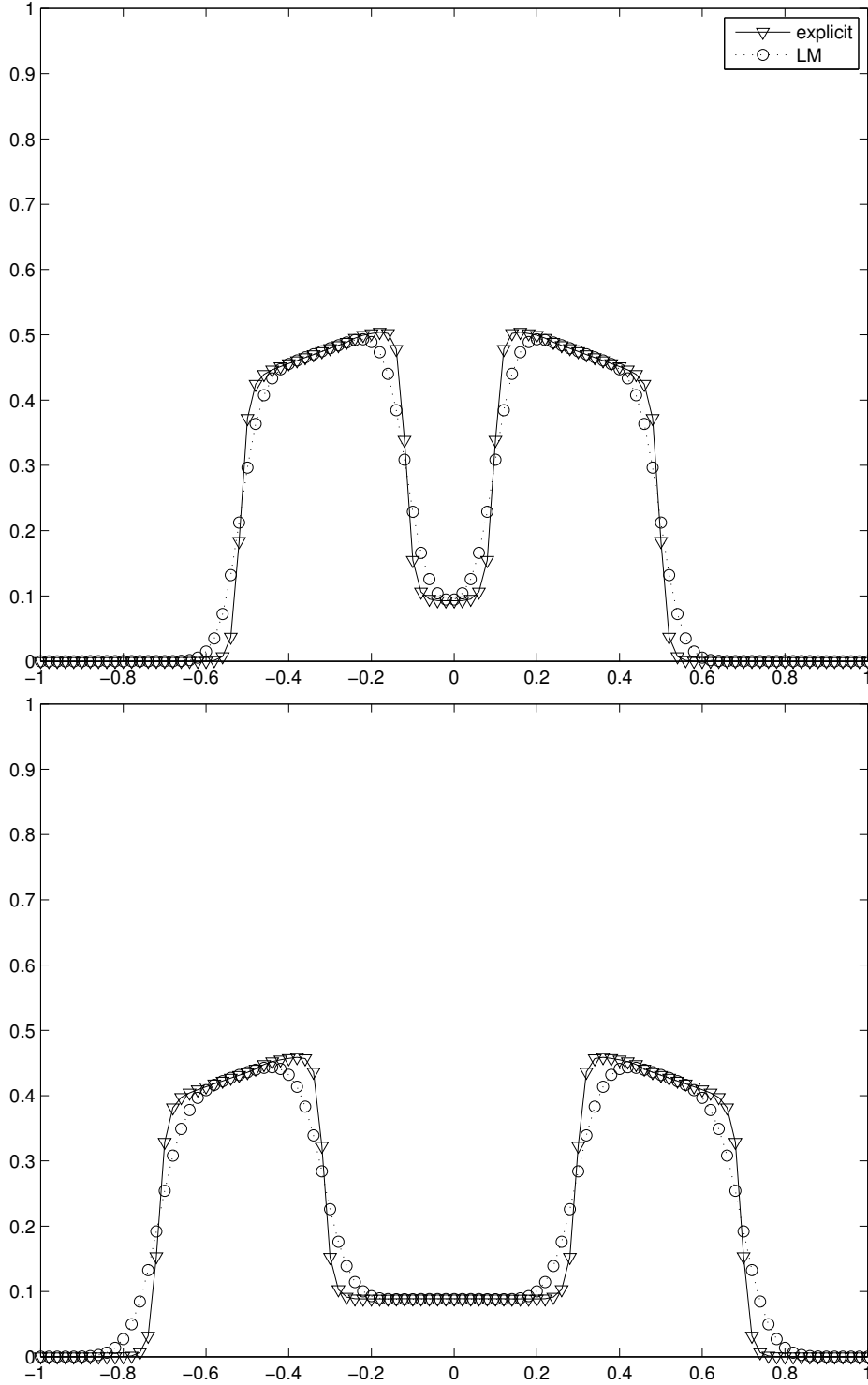
Figure 2: Telegraph equation $\varepsilon = 1$: comparison between explicit and LM schemes: $t = 3/10$ (top), $t = 5/10$ (bottom).
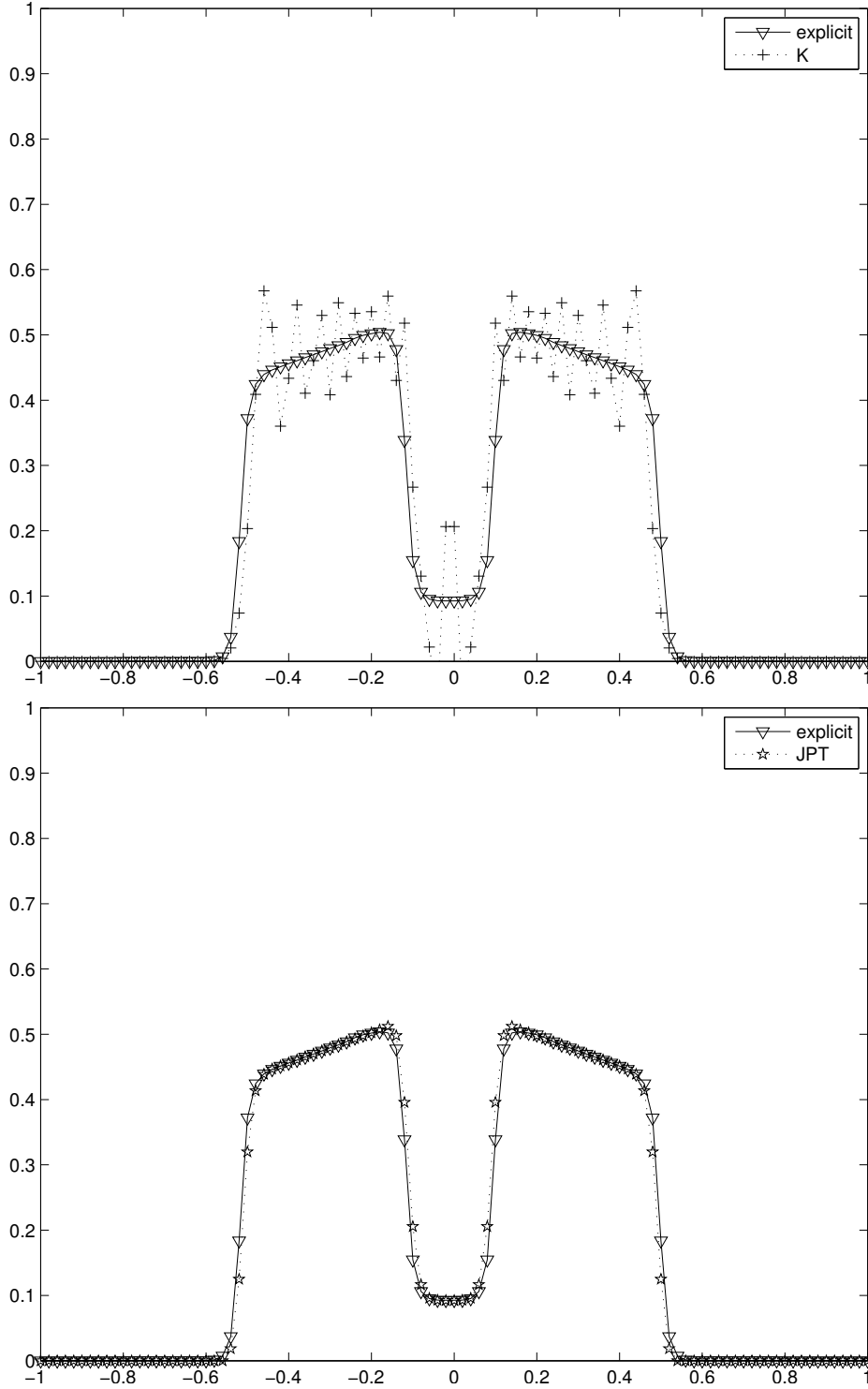
Figure 3: Telegraph equation $\varepsilon = 1$, $t = 3/10$: comparison between explicit and K schemes (top), and between explicit and JPT schemes (bottom).
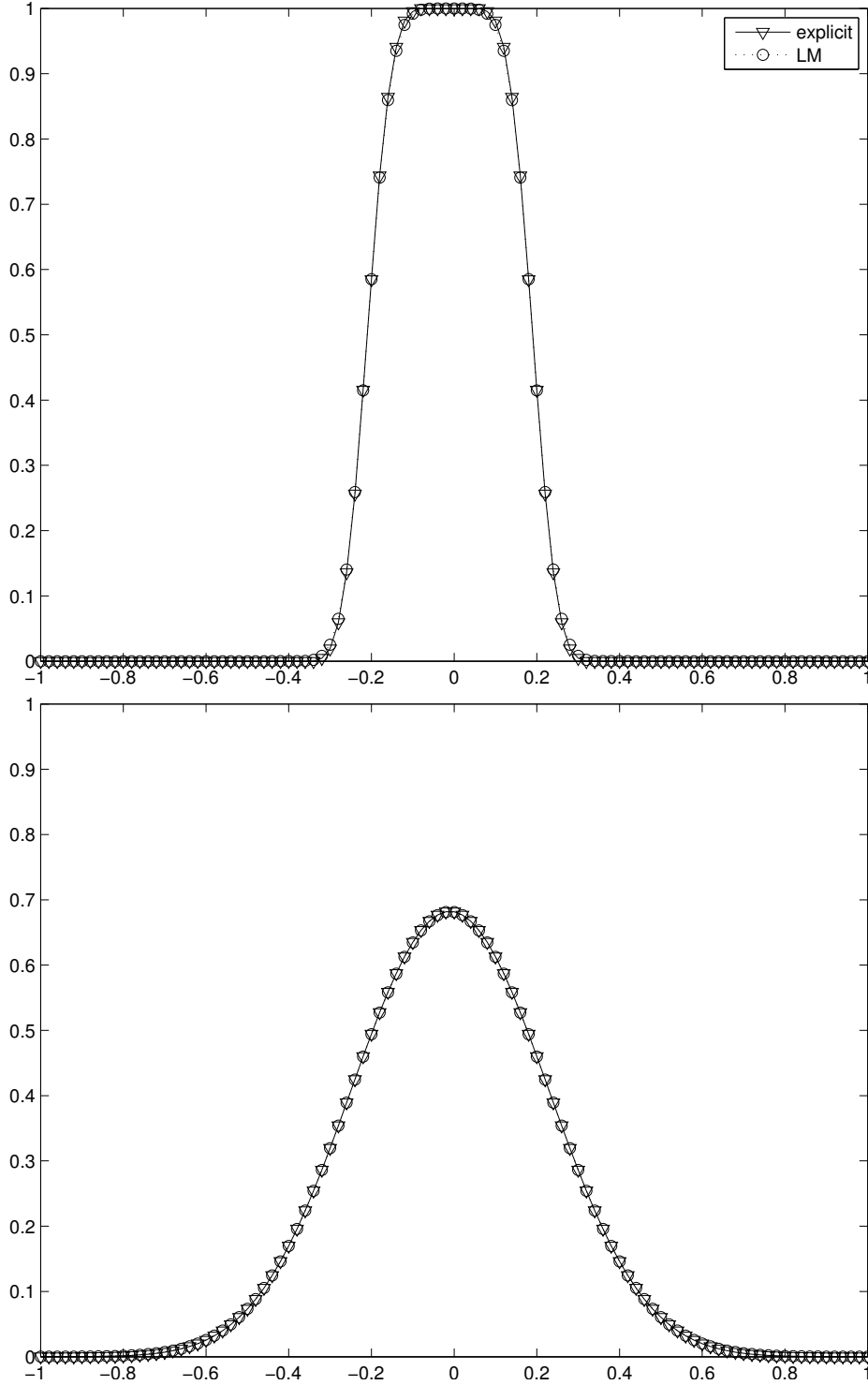
Figure 4: Telegraph equation $\varepsilon = 10^{-10}$: comparison between diffusion and LM schemes: $t = \varepsilon/100$ (top), $t = 2\varepsilon/10$ (bottom).
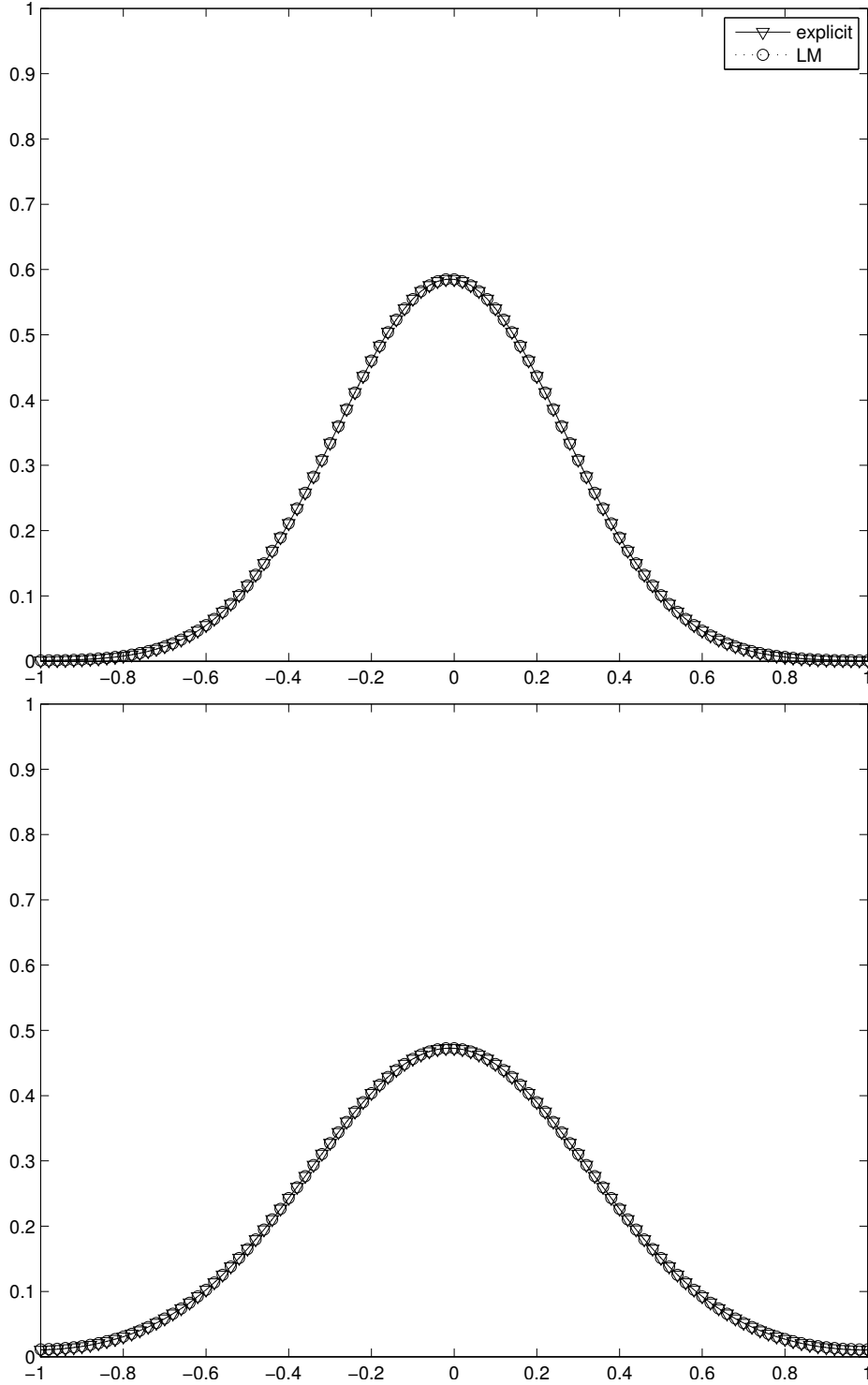
Figure 5: Telegraph equation $\varepsilon = 10^{-10}$: comparison between diffusion and LM schemes: $t = 3\varepsilon/10$ (top), $t = 5\varepsilon/10$ (bottom).
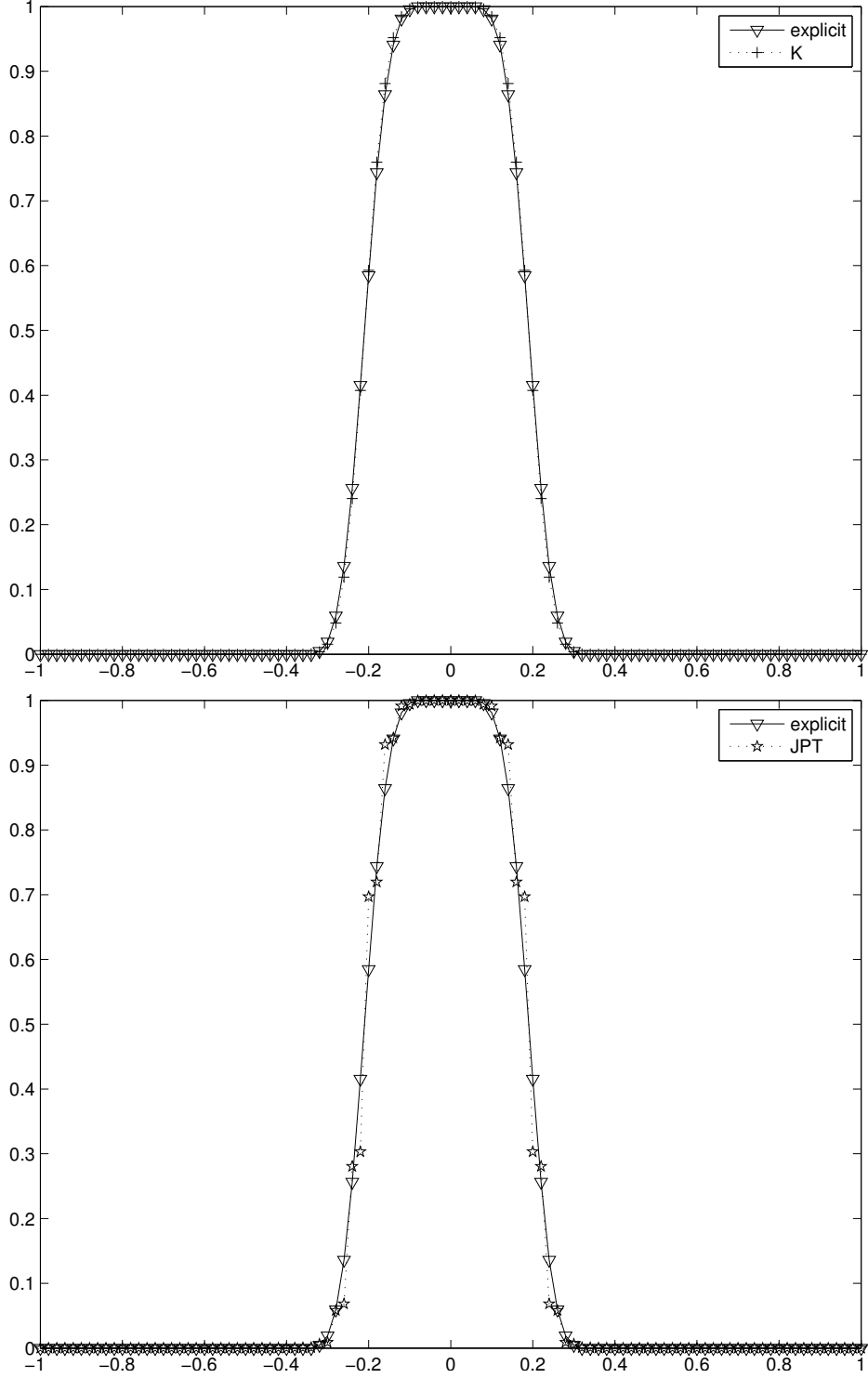
Figure 6: Telegraph equation $\varepsilon = 10^{-10}$, $t = \varepsilon/100$: comparison between diffusion and K schemes (top), and between diffusion and JPT schemes (bottom).
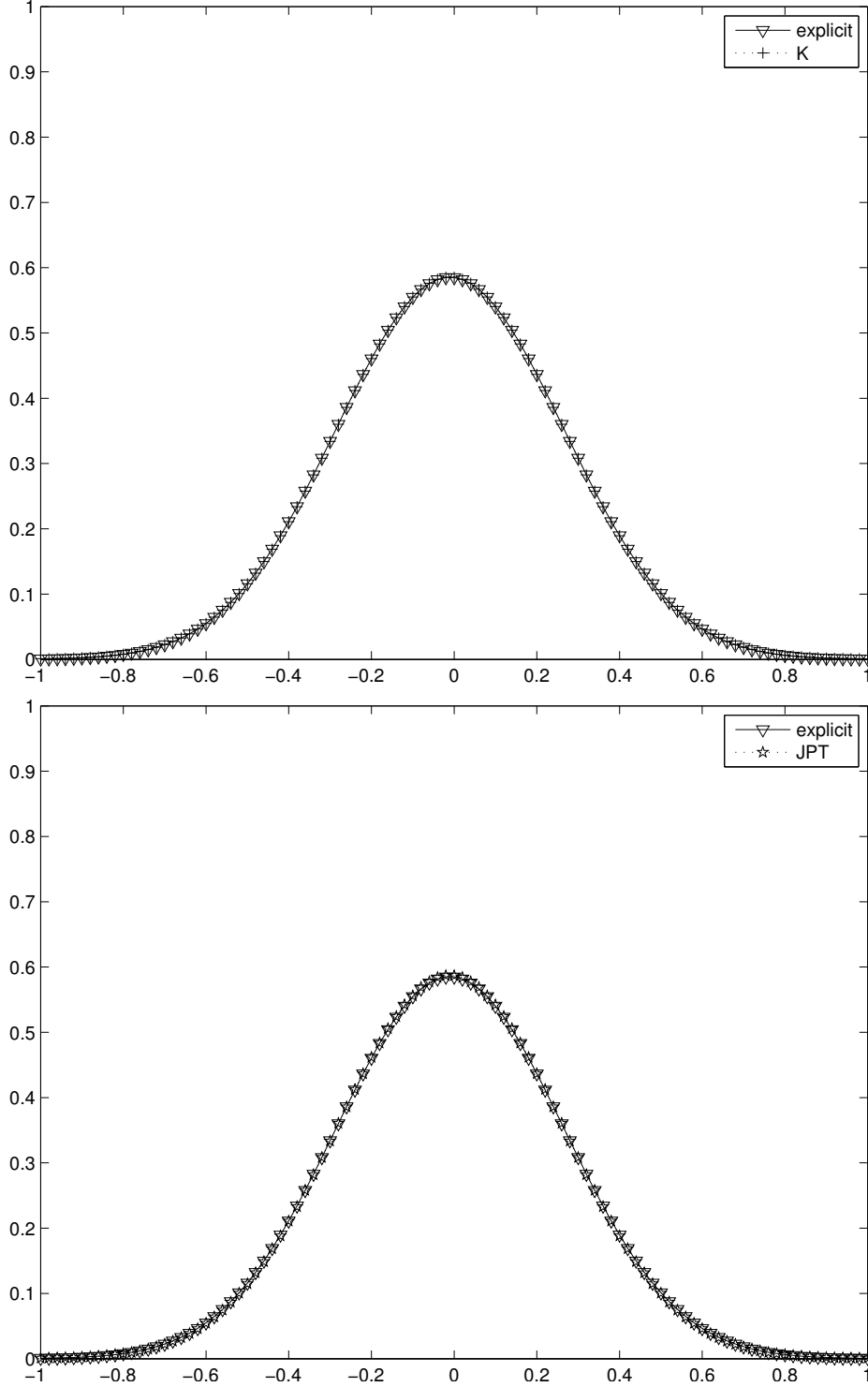
Figure 7: Telegraph equation $\varepsilon = 10^{-10}$, $t = 3\varepsilon/10$: comparison between diffusion and K schemes (top), and between diffusion and JPT schemes (bottom).
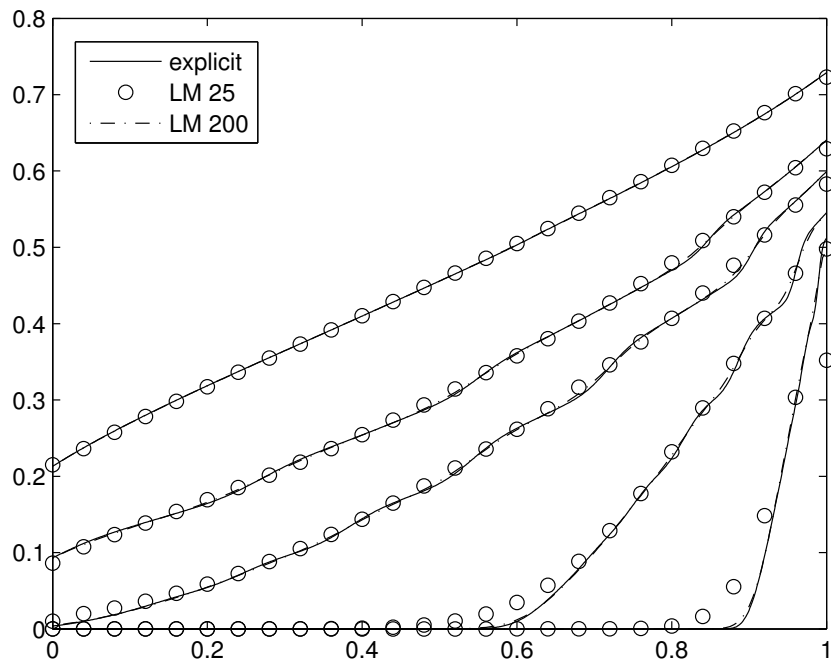
Figure 8: One groupe transport equation - Example 1: comparison between explicit and LM schemes (25 and 200 grid points). Results at times $t = 0.1$, 0.4, 1.0, 1.6 and 4 ($\varepsilon = 1$).
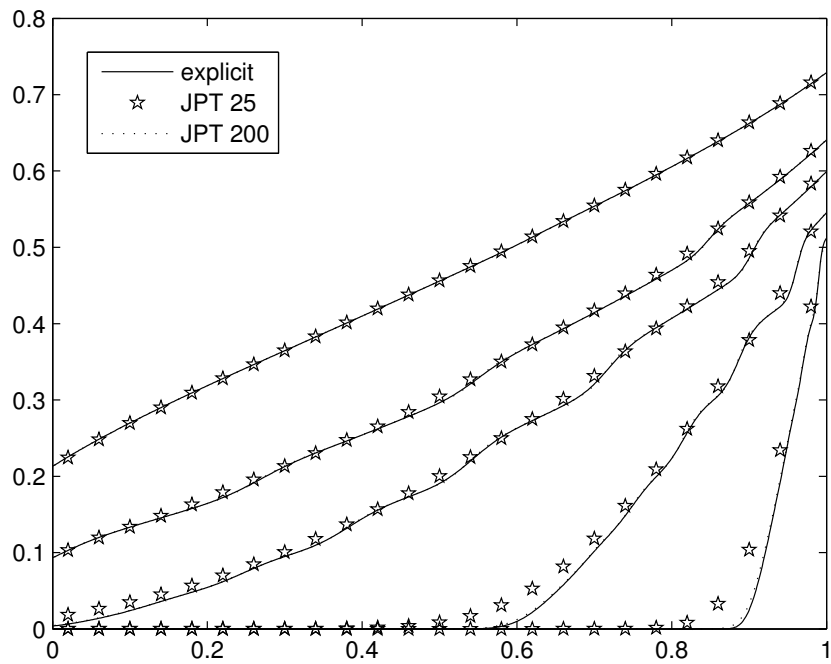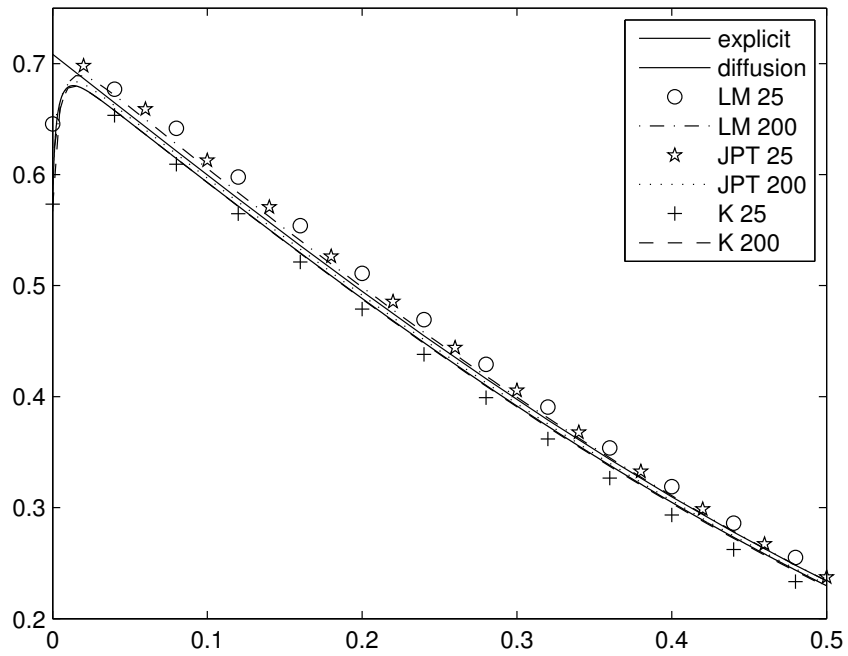
Figure 9: One groupe transport equation - Example 1: comparison between explicit and JPT schemes (25 and 200 grid points) . Results at times $t = 0.1$, 0.4, 1.0, 1.6 and 4 ($\varepsilon = 1$).
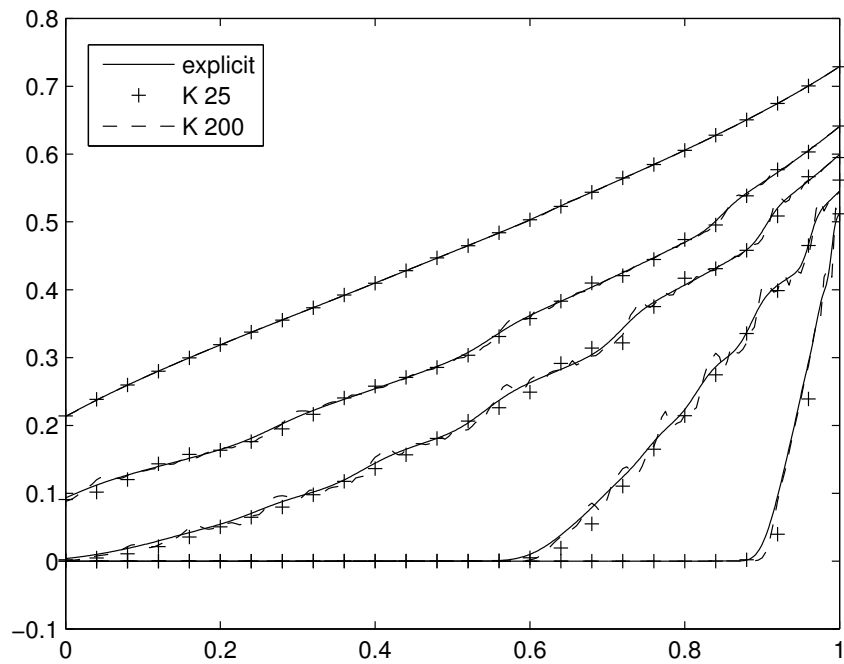
Figure 10: One groupe transport equation - Example 1: comparison between explicit and K schemes (25 and 200 grid points). Results at times $t = 0.1$, 0.4, 1.0, 1.6 and 4 ($\varepsilon = 1$).
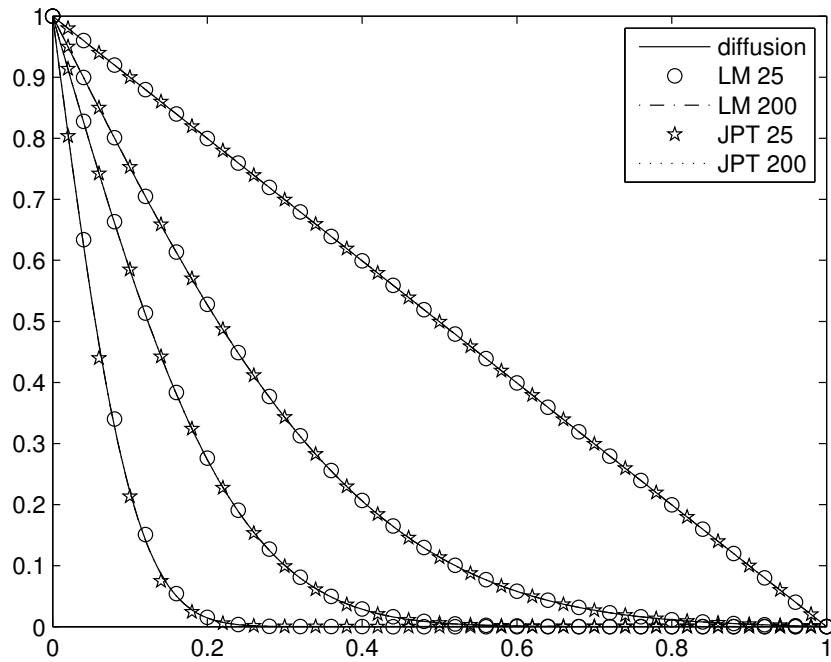
Figure 11: One groupe transport equation - Example 2: comparison between diffusion solution and LM and JPT schemes (25 and 200 grid points). Results at times $t = 0.01$, 0.05, 0.15 and 2 ($\varepsilon = 10^{-8}$).
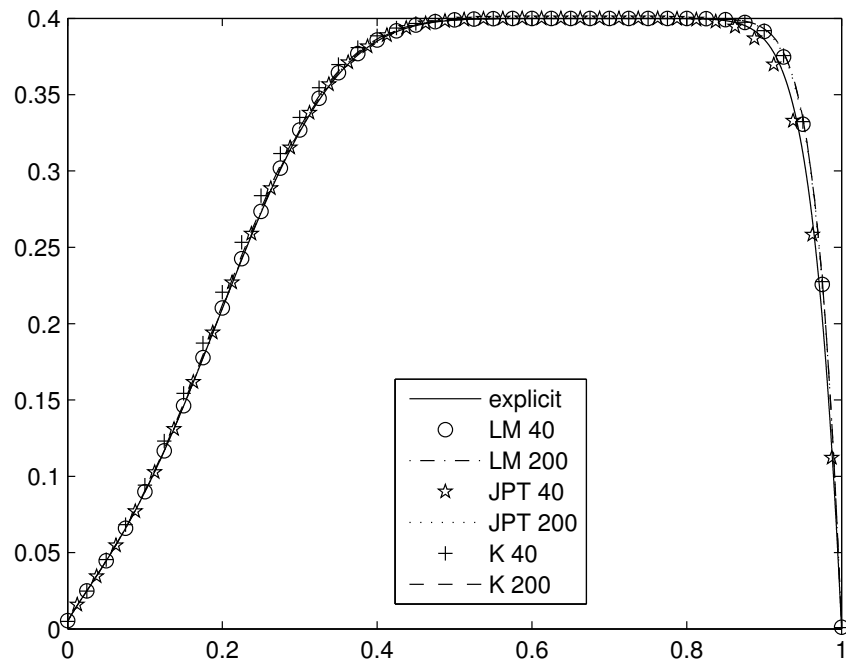
Figure 12: One groupe transport equation - Example 3: comparison between explicit scheme and schemes LM, JPT, and K (40 and 200 grid points).

Figure 13: One groupe transport equation - Example 4: comparison between explicit scheme (solid line with boundary layer), diffusion solution (solid straight line), and schemes LM, JPT, and K (25 and 200 grid points) ($\varepsilon = 10^{-2}$).
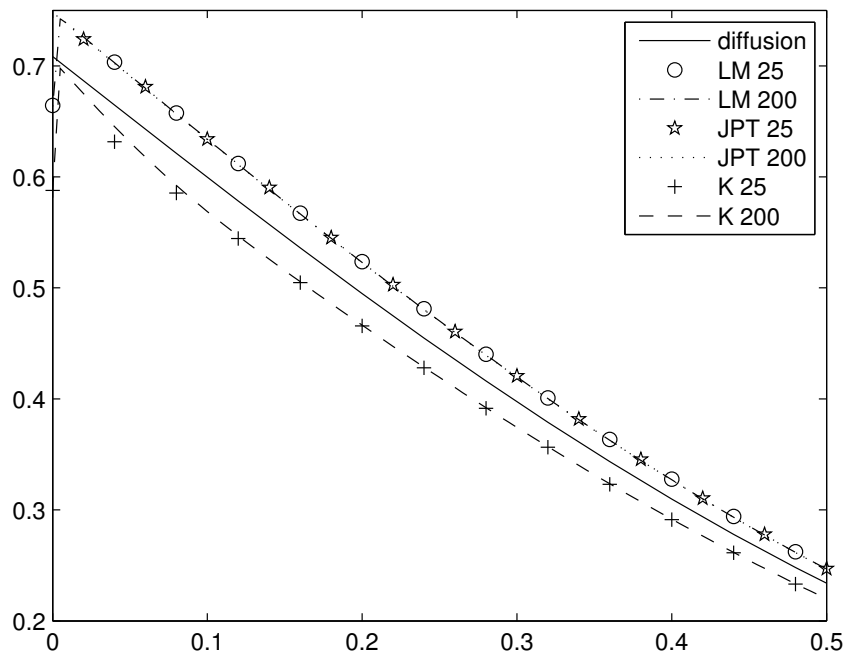
Figure 14: One groupe transport equation - Example 5. Comparison between diffusion solution and schemes LM, JPT, and K (25 and 200 grid points) ($\varepsilon = 10^{-4}$).
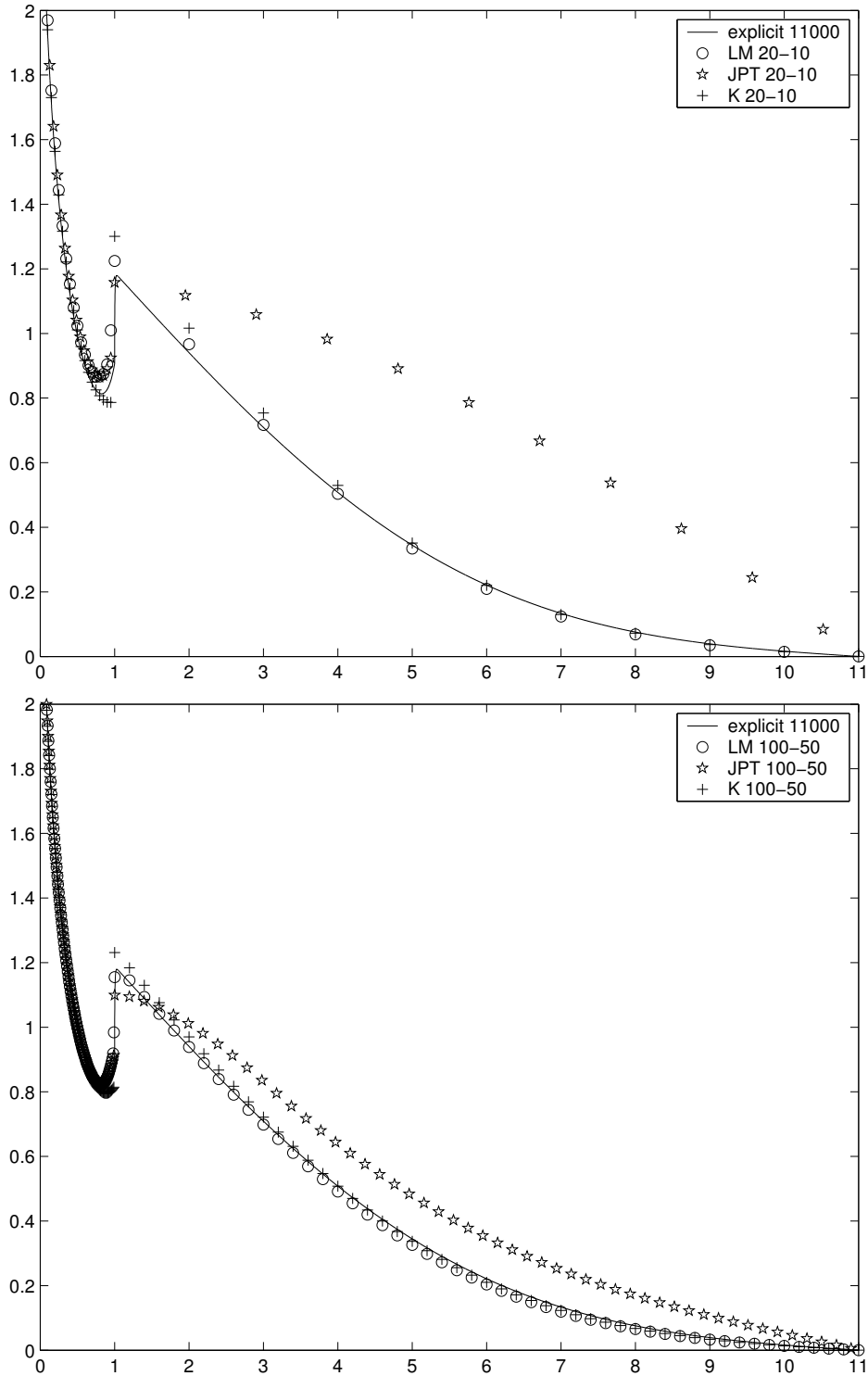
Figure 15: One groupe transport equation - Example 6. Comparison between reference solution and schemes LM, JPT, and K with a coarse mesh (top) and a thin mesh (bottom), at time $t = 2000$.
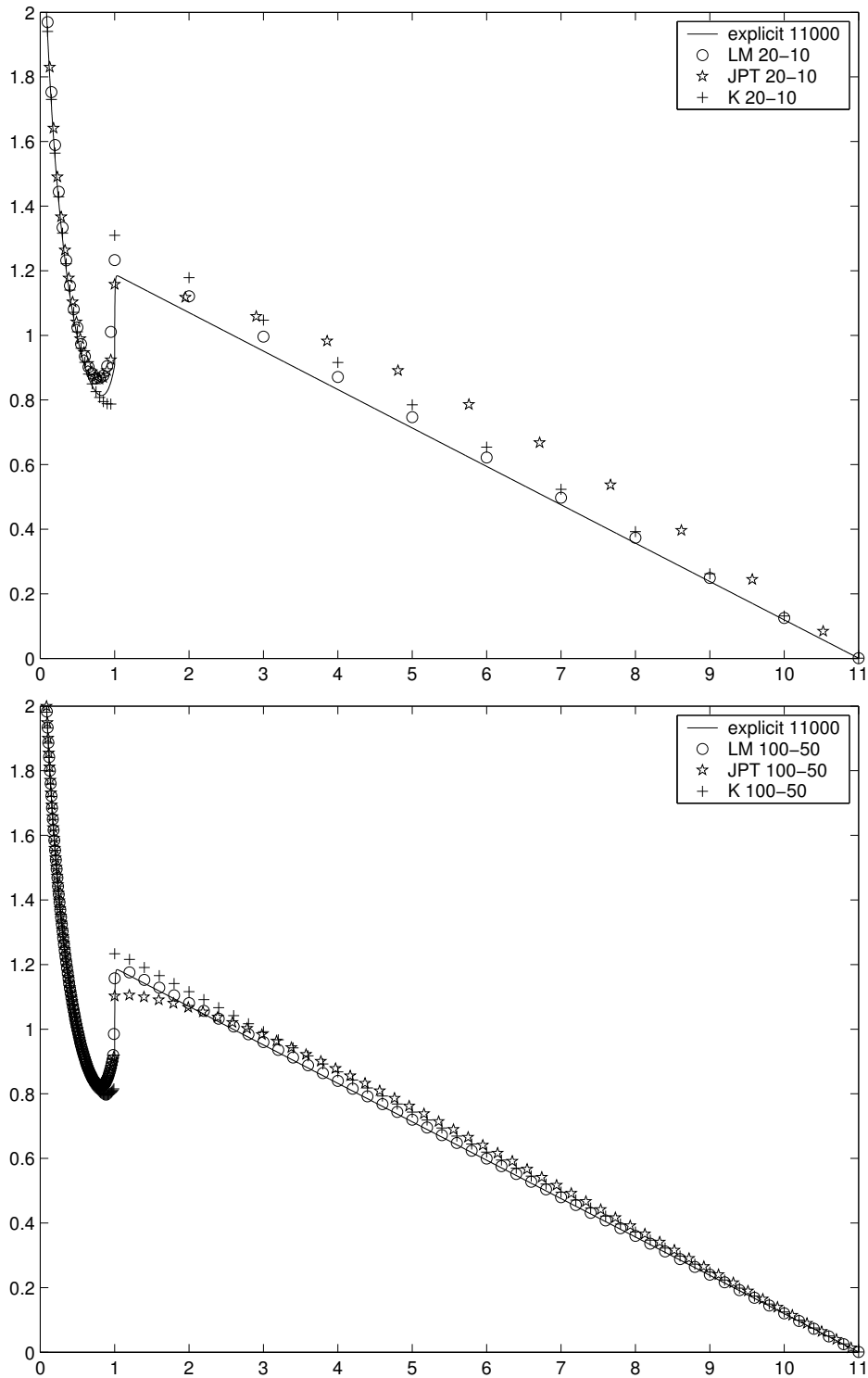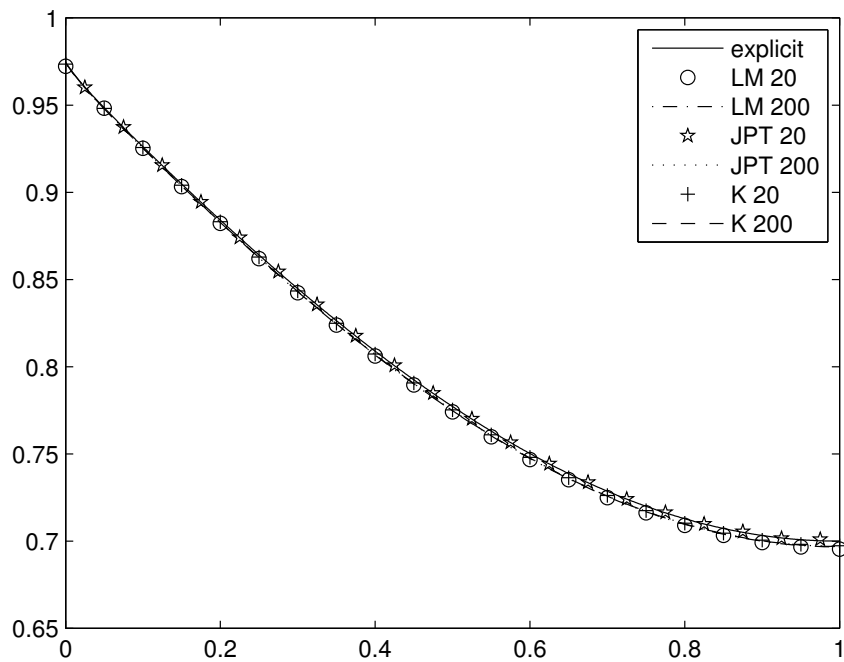
Figure 16: One groupe transport equation - Example 6. Comparison between reference solution and schemes LM, JPT, and K with a coarse mesh (top) and a thin mesh (bottom), at steady state.
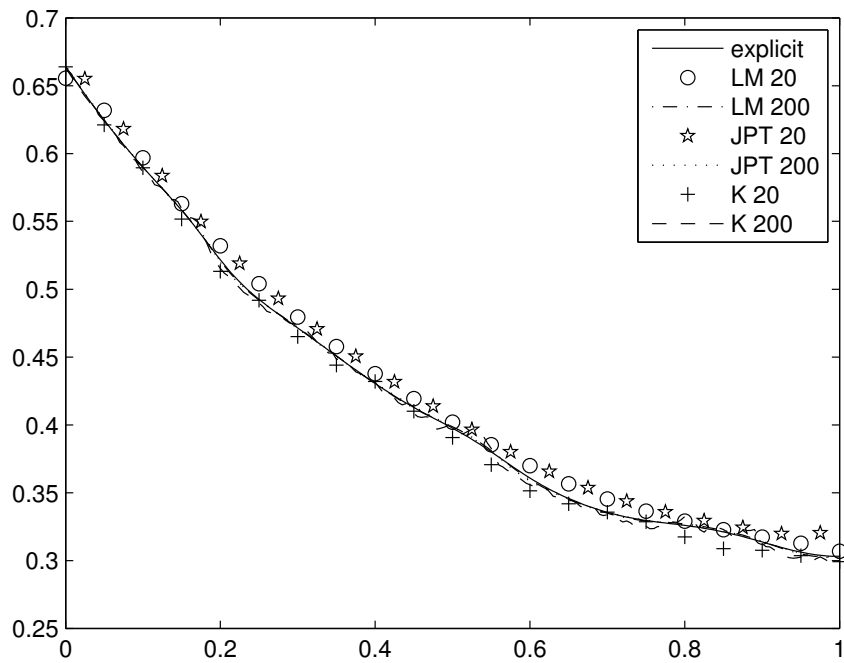
Figure 17: One groupe transport equation - Example 7: comparison between reference solution and schemes LM, JPT, and K (20 and 200 grid points), $\varepsilon = 1$ (top) and $\varepsilon = 0.1$ (bottom).
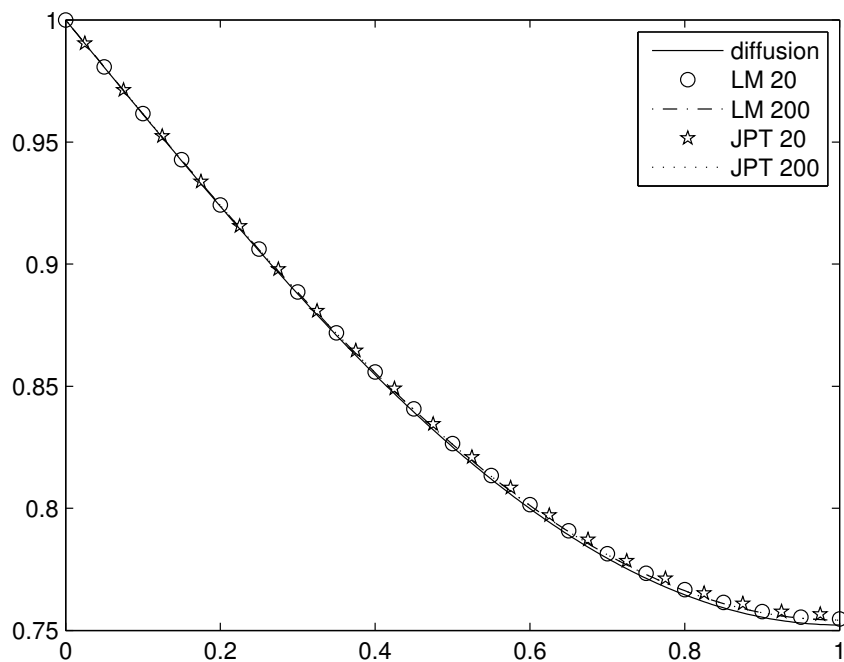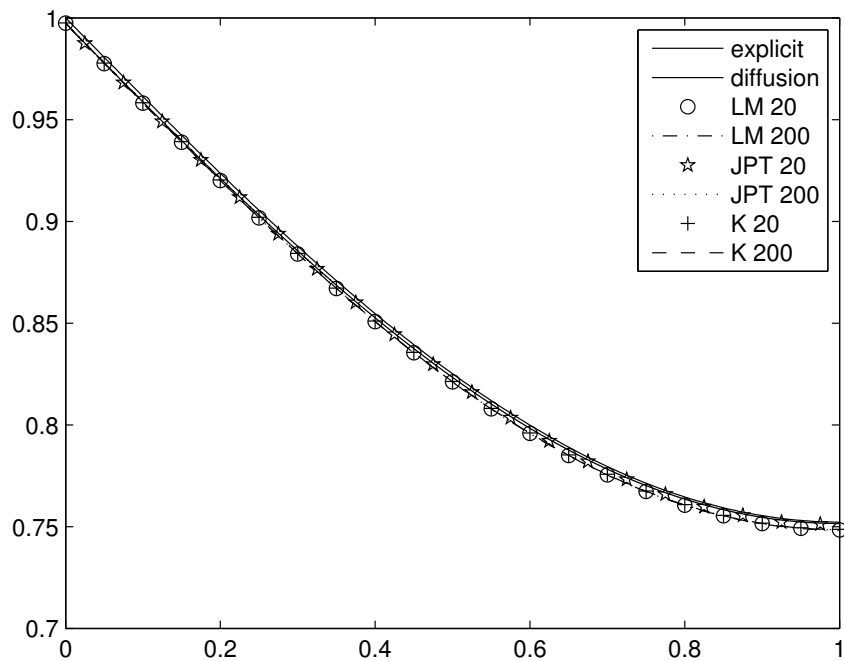
Figure 18: One groupe transport equation - Example 7: comparison between reference solution and schemes LM, JPT, and K (20 and 200 grid points), $\varepsilon = 0.01$ (top) and $\varepsilon = 10^{-10}$ (bottom).